

NACA RM E50F15

6093

E 50 F 15

TECH LIBRARY KAFB, NM
0143615

~~53 29 55~~
NACA

RESEARCH MEMORANDUM

PRELIMINARY CORRELATION OF EFFICIENCY OF AIRCRAFT
GAS-TURBINE COMBUSTORS FOR DIFFERENT
OPERATING CONDITIONS

By J. Howard Childs

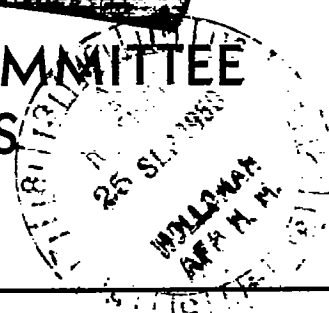
Lewis Flight Propulsion Laboratory
Cleveland, Ohio

JHC
CLASSIFIED DOCUMENT

Information affecting the National Defense of the United States within the meaning of the Espionage Laws, Title 18, U.S.C., Sec. 793 and 794, the transmission or the revelation of its contents in any manner to an unauthorized person is prohibited by law.
Information so classified may be imparted only to those personnel in the Army, Navy, Air Force, and Marine Corps who have a legitimate interest therein, and to United States citizens of known loyalty and discretion who are authorized to receive such information.

**NATIONAL ADVISORY COMMITTEE
FOR AERONAUTICS**

WASHINGTON
September 21, 1950



CONFIDENTIAL

319.98/13



0143615

NACA RM E50F15



NATIONAL ADVISORY COMMITTEE FOR AERONAUTICS

RESEARCH MEMORANDUM

PRELIMINARY CORRELATION OF EFFICIENCY OF AIRCRAFT GAS-TURBINE
COMBUSTORS FOR DIFFERENT OPERATING CONDITIONS

By J. Howard Childs

SUMMARY

An empirical correlation is presented of the combustion-efficiency data previously obtained in experimental investigations with 14 aircraft gas-turbine combustors. The precision of the correlations is not good for some of the combustors. The correlations are of value, however, in predicting the efficiency at different operating conditions and in comparing the performance of different combustors from data obtained in unrelated tests.

A theoretical analysis based on the kinetics of a bimolecular chemical reaction is also presented which, with additional assumptions regarding the mechanism of the combustion process, yields the correlation parameter previously obtained by empirical means. The theoretical analysis yields equations that predict the shape of the curves obtained by plotting the experimental data.

INTRODUCTION

Investigations of the performance of various gas-turbine combustors at the NACA Lewis laboratory have yielded a large amount of combustor performance data, but no method has been presented for correlating these data in terms of fundamental parameters. Reference 1 showed that combustion efficiency and maximum obtainable temperature rise were decreased by a decrease in combustor-inlet pressure or temperature and by an increase in combustor-inlet velocity. No parameter was expressed, however, for combining these effects to make possible a prediction of combustor performance for any given operating conditions.

A parameter was derived by empirical methods which served to correlate these data, and the correlations are presented herein. A theoretical analysis of the combustion process was also made to illustrate that the empirically-derived parameter could also be

CONFIDENTIAL



derived from a theoretical approach. This work was carried out simultaneously with the experimental phases of the research. The theoretical analysis and methods of correlating combustor performance data that are presented in this report were arrived at as early as 1944. Attempts to refine the analysis and the use of entirely different theoretical analyses have failed to yield a better means of correlating the experimental data. The method of correlating combustor performance data that is presented herein is therefore as good as could readily be achieved with presently available experimental data and with the present knowledge of the combustion process.

ANALYSIS

Empirical. - The data of reference 1 show that the combustion efficiency is affected by combustor-inlet pressure, temperature, and velocity in a manner that later investigations proved to be characteristic of all gas-turbine combustors. In reference 1 combustion efficiencies are recorded when each of these three variables is independently altered. With these data, the log of the combustion efficiency is plotted against the log of each of the three variables. The slopes of the resulting lines show the manner of variation of the efficiency with each of these variables. The significant parameter that resulted from this empirical analysis is $P_1 T_1 / V_r$. In this parameter, P_1 is the combustor-inlet static pressure in pounds per square foot absolute; T_1 , the combustor-inlet static temperature in $^{\circ}\text{R}$; and V_r , the combustor reference velocity in feet per second computed from the total air mass flow rate, P_1 , T_1 , and the maximum cross-sectional area of the combustor flow passage. Combustion efficiency η_b is correlated as a function of $P_1 T_1 / V_r$.

Theoretical. - A further analysis was made to illustrate that the data correlations could be predicted from theoretical considerations.

A theoretical treatment of gas-turbine combustion is difficult because of the many different processes that occur in the combustors. The fuel must be vaporized, mixed with air, ignited, and oxidized to the final products of combustion. These combustion products must then be mixed with dilution air to reduce the temperatures to values that can be tolerated by the turbine blades. The combustion can be visualized as a competition between the conversion processes (vaporization, mixing, ignition, and oxidation) and the quenching that occurs when the reacting mixture is cooled and diluted by the dilution air and when the reacting mixture comes in contact with the

relatively cool walls of the combustor liner. If the rate of any one of the conversion processes is substantially less than the rates of the others, this one process will govern the over-all rate and hence will determine the combustion efficiency. The relative rates of the conversion processes can be expected to change as combustor operating conditions are changed, and thus it may be that entirely different processes or different combinations of processes will determine the combustion efficiency at widely different operating conditions.

The theoretical analysis was based on the assumption that the chemical reaction (the oxidation of the fuel) constitutes an over-all rate-determining step in the combustion. This oxidation probably occurs by a chain mechanism. It is frequently true, however, that the kinetics of chain reactions are dependent entirely upon the kinetics of a single, slowly occurring reaction within the chain. The analysis was therefore based on the kinetics of a bimolecular chemical reaction. Additional simplifying assumptions were required in order to obtain from this analysis the parameter $P_1 T_1 / V_r$ previously derived by empirical methods. The theoretical analysis is presented in detail in the appendix, where the symbols used herein are defined. The final equations resulting from that analysis are as follows:

$$\ln \frac{1 - \frac{N_A}{N_B} \eta_b}{1 - \eta_b} + K_5 = K_{10} \frac{P_1 T_1}{V_r} \quad (1)$$

$$\frac{\eta_b}{1 - \eta_b} + K_6 = K_{11} \frac{P_1 T_1}{V_r} \quad (2)$$

$$\eta_b = f \left(\frac{P_1 T_1}{V_r} \right) \quad (3)$$

where N_A and N_B are the concentrations of the two reactants in the bimolecular chemical reaction; and K_5 , K_6 , K_{10} , and K_{11} are constants. Equation (1) applies for a given combustor operating with a single fuel at a fixed fuel-air ratio for the general case where $N_A < N_B$. Equation (2) should apply for the same conditions of operation only if the combustion occurs in a zone where $N_A = N_B$. Equation (3) is a general statement of either of the preceding two equations.

The arbitrary assumptions on which the theoretical analysis is based are as follows:

(1) Some bimolecular chemical reaction is the over-all rate-controlling step in combustion.

(2) The temperature T in the reaction zone is constant. This assumption renders constant the important kinetics term $e^{-E/RT}$, where E is the energy of activation for the chemical reaction and R is the gas constant.

(3) The volume of the reaction zone does not change with a change in operating conditions.

RESULTS AND DISCUSSION

Figures 1 to 14 show values of combustion efficiency η_b for 14 different aircraft gas-turbine combustors plotted against the parameter $P_1 T_1 / V_r$ in accordance with equation (3). The parameter $P_1 T_1 / V_r$ is equivalent to a dimensional constant times the parameter P_1^2 / W_a where W_a is the air mass flow rate. These combustor performance data were obtained from NACA experimental investigations with these combustors. The different combustors are given letter designations in figures 1 to 14, and most of the combustors are not described herein. Several combustors of both the annular and tubular types are included, and some of these are from current production engines. The data for figure 1 were taken from reference 1 by reading values of η_b from the faired curves (fig. 8 of reference 1) at each of four fuel-air ratios (0.011, 0.013, 0.015, and 0.017). The data for the other combustors (figs. 2 to 14) were computed from the original test data, using each individual data point. The data of figures 1 to 14 are therefore for a range of fuel-air ratios.

The precision of the data correlations for most of the combustors is not good. Some scatter of the data points is to be expected, however, inasmuch as it is seldom possible to accurately reproduce values of η_b in day-to-day operation at the same test conditions. In repeated check tests at identical operating conditions, values of η_b differing by 4 percent are encountered with most combustors, and at very severe operating conditions the values of η_b have been observed to differ as much as 10 percent with many combustors. For the combustor of reference 1, values of η_b may differ as much as 17 percent at identical operating conditions owing to the

tendency of this combustor to follow two different operating curves. (See figs. 8(b) and 8(c) of reference 1.) It has not been established that other combustors follow such dual operating curves, but it is suspected that some of them do. A correlation of experimental values of η_b that for most combustors gives a maximum scatter of ± 2 percent at favorable operating conditions and ± 5 percent at severe operating conditions is therefore as good as can possibly be achieved. A criterion for a good correlation might be ± 3 -percent maximum data scatter at favorable operating conditions and ± 7 -percent at severe conditions. In view of these considerations, the data correlations of figures 3 and 4 appear good, inasmuch as only a few data points exceed the allowable ± 7 percent deviation at severe operating conditions. The data scatter in figures 7 and 8 is so great, however, that the correlation is of little value.

When the parameter $P_i T_i / V_r$ is used to correlate combustor performance data, a separate curve might be expected for each fuel-air ratio. Most combustors, however, give a substantially constant efficiency for a range of fuel-air ratios (this is evident in the curves of fig. 8 of reference 1) and thus the experimental data for most fuel-air ratios fall on a single mean curve in figures 1 to 14. At very high and very low fuel-air ratios, the efficiencies are generally lower than at intermediate fuel-air ratios. The parameter $P_i T_i / V_r$ does not correct for this effect, and some of the data scatter in the figures is due to this phenomenon.

For each of the combustors the curves of figures 1 to 14 have the same general shape. At high values of the parameter $P_i T_i / V_r$, combustor performance is quite satisfactory; the combustion efficiency is high and is not very sensitive to changes in operating conditions, as evidenced by the gradual slope of the curves. At low values of $P_i T_i / V_r$, however, combustor performance is not satisfactory; the efficiency is low and decreases rapidly as $P_i T_i / V_r$ decreases. This characteristic shape of the performance curves leads to the concept of a critical value of $P_i T_i / V_r$, which separates the satisfactory from the unsatisfactory range of operating conditions. For each combustor the critical value of $P_i T_i / V_r$ is arbitrarily selected as the value corresponding to $\eta_b = 0.85$ on the curves of figures 1 to 14.

These critical values of $P_1 T_1 / V_r$ can be used to form a rating scale that will indicate the relative abilities of different combustors to perform satisfactorily at severe (low $P_1 T_1 / V_r$) operating conditions. The better combustors will have lower values of critical $P_1 T_1 / V_r$. Table I presents such a rating scale with the 14 combustors listed in order of increasing critical $P_1 T_1 / V_r$. The combustion efficiency of a gas-turbine engine at altitude can be improved without an attendant increase in engine frontal area by replacing the combustor with another combustor that is higher on the rating scale in table I.

Inspection of figures 1 to 14 shows that for values of $P_1 T_1 / V_r$ below the critical ($\eta_b < 0.85$), the slopes of the curves of η_b against $P_1 T_1 / V_r$ are in general greater for those combustors having lower critical values of $P_1 T_1 / V_r$. This trend might be expected; absolute pressure limits of inflammability exist, and the combustors of better design merely extend the range of $P_1 T_1 / V_r$ for which they give high values of η_b closer to these limits.

Equations (1) and (2) are of different form; equation (1) holds for the general case where $N_A < N_B$, and equation (2) should be valid only for the special case where $N_A = N_B$. Figure 15 shows the data of figure 3 plotted so as to obtain the straight-line relation expressed by equation (1); that is, the log of the function

$\left(1 - \frac{N_A}{N_B} \eta_b\right) / (1 - \eta_b)$ is plotted against the parameter $P_1 T_1 / V_r$ for two arbitrary values of the ratio N_A / N_B ($N_A / N_B = 1/2$ and $1/4$).

The predicted straight-line correlation is obtained with either value of the ratio N_A / N_B . Figure 16 shows these same data plotted in accordance with equation (2). The data do not fall on a straight line; equation (2) therefore does not apply and hence the reaction does not occur in a zone where $N_A = N_B$, which is in accord with probability considerations.

The fact that the straight-line relation predicted by equation (1) is actually obtained in figure 15 means that equation (1) is of the proper form and predicts the shape of the experimental curves; this lends credence to the theoretical analysis that yielded equation (1). It is emphasized, nevertheless, that the theoretical analysis is not of such a nature as to establish definitely chemical-reaction kinetics as the over-all rate-controlling factor in the combustion. Several arbitrary assumptions were required in order to

1353

CONFIDENTIAL

NACA RM E50F15

7

arrive at the parameter $P_1 T_1 / V_r$. It might be possible to derive a parameter that will correlate the data by means of a theoretical analysis entirely different from that presented herein; such a parameter, to be successful, would have to be quite similar to $P_1 T_1 / V_r$, and the equations would have to be a form of the second-order law like those derived herein.

Attempts have been made to correlate combustor performance data by using parameters derived from each of the assumptions that: (1) fuel vaporization, (2) mixing by molecular diffusion, (3) mixing by turbulent eddy diffusion, and (4) quenching by wall contact control the over-all rate of combustion. The parameters based on each of these assumptions gave no correlation whatsoever of the experimental data. Attempts have also been made (using empirical methods) to refine the equations presented herein so as to obtain better correlation of the data; no substantial improvements in the correlations have been achieved, however. It is therefore concluded that the data correlations presented herein are as good as can be readily obtained with the present knowledge of the combustion process and with presently available performance data.

Data that establish the importance of fuel atomization in the combustion process are available, as, for example, reference 2. These data indicate that vaporization of the fuel may play a rate-determining role. The differences in fuel atomization resulting from the use of different injection nozzles may serve primarily to alter the volume of the combustion zone, however, and thus such data do not necessarily invalidate the analysis presented herein.

Lewis Flight Propulsion Laboratory,
National Advisory Committee for Aeronautics,
Cleveland, Ohio.

APPENDIX

THEORETICAL ANALYSIS OF TURBINE-ENGINE

COMBUSTION PROCESS

Fuel atomization, dispersion, and vaporization, mixing of the fuel and primary air, ignition, oxidation of the fuel by a chain mechanism, and quenching and dilution by secondary air are important phases of the combustion process in gas-turbine combustors. For certain ranges of operating conditions it is possible that the oxidation process, or more specifically one step in the oxidation chain, governs the over-all rate at which combustion proceeds. The analysis is therefore based on the kinetics of a bimolecular reaction; that is, a reaction involving the collision of two molecules. The range of operating conditions for which combustor performance data satisfy the equations will indicate the range for which chemical kinetics, as applied in this particular analysis, may govern the over-all combustion rate.

Outline of Analysis

A simplified derivation of the necessary kinetics equation is first made. This derivation is similar to those appearing in textbooks on reaction kinetics (for example, reference 3). Such simplified derivations involve assumptions and approximations; reference 4 presents a rigorous derivation of these equations. The kinetics equations are then applied to the case of a typical gas turbine combustor, and the variables in the equations are replaced by variables that are measured in combustor investigations. Finally, performance data obtained with aircraft gas-turbine combustors are plotted in accordance with the derived equations.

Symbols

The symbols used in the analysis are as follows:

- A_a average cross-sectional area of reaction zone, sq ft
- A_r maximum cross-sectional area of combustor flow passage, sq ft
- E energy of activation for reaction, ft-lb/lb

NACA RM E50F15

9

$K_1, K_2,$ $K_3, \text{ etc.}$	constants
$\frac{dw}{d\theta}$	reaction rate, lb mixture reacting/(sec)(cu ft)
z	distance from upstream end of reaction zone to plane of any point within reaction zone, ft
L	length of reaction zone, ft
n	number of molecules per cubic foot, cu ft ⁻¹
N	number of molecules per pound original mixture, lb ⁻¹
P	static pressure, lb/sq ft abs.
R	gas constant, ft-lb/(lb)(°R)
T	absolute static temperature, °R
u	mean molecular velocity, ft/sec
V_a	velocity based on density, mass flow, and average cross-sectional area of reaction zone, ft/sec
V_r	velocity based on combustor-inlet density, total air flow, and maximum cross-sectional area of combustor flow passage, ft/sec
X	fraction of N reacted at any time θ or at any location within combustor
Z	number of molecular collisions of type involved in reaction, per unit volume per unit time, ft ⁻³ sec ⁻¹
α	probability factor, fraction of collisions involving sufficient energy for reaction to occur which actually result in a reaction
η_b	combustion efficiency
θ	time, sec

CONFIDENTIAL

~~CONFIDENTIAL~~

- ρ density, lb/cu ft
 σ effective molecular diameter, ft
 ϕ fraction of collisions involving sufficient energy for reaction to occur

1353

Subscripts:

- A reactant A in reaction $A+B \rightarrow C+D$
 B reactant B in reaction $A+B \rightarrow C+D$
 i combustor inlet

Simplified Derivation of Kinetics Equations

For the bimolecular reaction



in which A is the reactant present in smaller quantity. The reaction rate is given by the equation

$$\frac{dw}{d\theta} = \frac{Z\phi}{N_A} \alpha \quad (A1)$$

The probability factor α will be assumed to be constant, which is conventional.

A molecular collision of the required type (A+B) occurs when the distance between the centers of the molecules is $(\sigma_A + \sigma_B)/2$. The average A molecule will therefore sweep out in unit time a cylindrical space of length u and having an effective cross section of $(\pi/4)(\sigma_A + \sigma_B)^2$. The number of collisions of the average A molecule with B molecules per unit time will be $(\pi/4)(\sigma_A + \sigma_B)^2 u n_B$. Each of the other A molecules is also colliding with B molecules; the total number of A+B collisions per unit time per unit volume is therefore

$$Z = \frac{\pi}{4} (\sigma_A + \sigma_B)^2 u n_A n_B$$

~~CONFIDENTIAL~~

Certain approximations are involved in this derivation, and when corrections are made for the distribution of molecular velocities and other factors, the equation becomes

$$Z = K_1 (\sigma_A + \sigma_B)^2 u n_A n_B \quad (A2)$$

By substituting $\sqrt{K_2 RT}$ for u , $\rho N_A (1-X)$ for n_A , and

$\rho N_B \left(1 - \frac{N_A}{N_B} X\right)$ for n_B ,

$$Z = K_3 (\sigma_A + \sigma_B)^2 (RT)^{1/2} (N_A N_B) (1-X) \left(1 - \frac{N_A}{N_B} X\right) \rho^2$$

When $\frac{P}{RT}$ is substituted for ρ ,

$$Z = \frac{K_3 (\sigma_A + \sigma_B)^2 N_A N_B (1-X) \left(1 - \frac{N_A}{N_B} X\right) P^2}{R^{3/2} T^{3/2}} \quad (A3)$$

From the Maxwell-Boltzman distribution law (references 3 and 4),

$$\varphi = e^{-E/RT} \quad (A4)$$

Equations (A3) and (A4) are substituted in (A1) to obtain

$$\frac{dw}{d\theta} = \frac{K_3 (\sigma_A + \sigma_B)^2 N_B (1-X) \left(1 - \frac{N_A}{N_B} X\right) P^2 e^{-E/RT}}{R^{3/2} T^{3/2}} \quad (A5)$$

Now

$$\frac{dX}{d\theta} = \frac{1}{\rho} \frac{dw}{d\theta} = \frac{K_3 (\sigma_A + \sigma_B)^2 N_B (1-X) \left(1 - \frac{N_A}{N_B} X\right) P e^{-E/RT}}{R^{1/2} T^{1/2}} \quad (A6)$$

The equations apply to any given sample of the reacting mixture as it passes through the combustor. The location of the sample and the value of X for the sample vary with time. At the outlet of

the reaction zone, X will equal η_b because the particular reaction under consideration is the one governing the over-all process. Thus,

$$X = \eta_b \quad \text{when } l = L \quad \text{and} \quad \theta = L/V_a \quad (A7)$$

and

$$X = 0 \quad \text{when } l = 0 \quad \text{and} \quad \theta = 0 \quad (A8)$$

It will now be assumed that the temperature in the zone where the reaction $A+B \rightarrow C+D$ occurs is substantially constant and independent of the combustor operating conditions and the combustion efficiency. Thus, T is constant. With this simplifying assumption it is possible to separate variables in equation (A6) and integrate

$$\frac{1}{1 - \frac{N_A}{N_B}} \ln \frac{1 - \frac{N_A}{N_B} X}{1 - X} + K_4 = \frac{K_3 (\sigma_A + \sigma_B)^2 N_B P \theta e^{-E/RT}}{R^{1/2} T^{1/2}} \quad (A9)$$

Rearranging terms and substituting from equation (A7), $X = \eta_b$ when $\theta = L/V_a$,

$$\ln \frac{1 - \frac{N_A}{N_B} \eta_b}{1 - \eta_b} + K_5 = \frac{K_3 (\sigma_A + \sigma_B)^2 (N_B - N_A) L P e^{-E/RT}}{V_a R^{1/2} T^{1/2}} \quad (A10)$$

A value of zero would be obtained for the constant K_5 by substituting the limits in equation (A8), $X = 0$ when $\theta = 0$, into equation (A10). This relation is not a true boundary condition for equation (A10), however, because at some operating conditions $X = 0$ when $\theta > 0$. Flame extinction or blow-out occurs whenever the velocity through the combustor exceeds a critical value, which is a function of the pressure, inlet temperature, and fuel-air ratio in the combustor (reference 1). At velocities above this critical value the quantity $\theta = L/V_a > 0$ and yet $X = 0$ since burning has ceased. The constant K_5 is therefore not equal to zero.

For the special case where the reaction $A+B \rightarrow C+D$ occurs in a zone where $N_A = N_B$ (stoichiometric for this particular reaction), equation (A6) integrates to

$$\frac{X}{1-X} + K_6 = \frac{K_3 (\sigma_A + \sigma_B)^2 N_B P \theta e^{-E/RT}}{R^{1/2} T^{1/2}} \quad (A11)$$

Substituting $X = \eta_b$ when $\theta = L/V_a$,

$$\frac{\eta_b}{1-\eta_b} + K_6 = \frac{K_3 (\sigma_A + \sigma_B)^2 N_B L P e^{-E/RT}}{V_a R^{1/2} T^{1/2}} \quad (A12)$$

Application to Typical Gas-Turbine Combustor

The foregoing equations are expressed in terms of the values of P , T , and V_a in the reaction zone. In experimental investigations these variables are not measured; the values of the combustor inlet variables P_i , T_i , and V_r , are usually determined however. The values of P , T , and V_a must therefore be expressed in terms of combustor-inlet conditions.

The pressure loss through a gas-turbine combustor is small compared with the inlet pressure, so the pressure P in the reaction zone is nearly equal P_i . In order to make some allowance for the difference between P and P_i , the following substitution is made

$$P = K_7 P_i \quad (A13)$$

Actually K_7 is not a constant, but it can be treated as such here by using a mean value for K_7 because its value never differs greatly from unity.

Between the combustor inlet and the zone where the reaction $A+B \rightarrow C+D$ occurs, the temperature of the mixture will markedly change owing to the processes of fuel vaporization, chemical reaction (the reactions preceding the particular one being considered in the analysis), and heat transfer to and from the surroundings. It has already been assumed that the particular reaction under consideration occurs at a substantially constant temperature so that

$$T = \text{constant} \quad (A14)$$

The value of V_a is given by the relation

$$V_a = K_8 K_9 V_r \frac{T}{T_1} \frac{P_1}{P} \quad (A15)$$

where K_8 is the fraction of the total air mass flow that passes through the reaction zone, and K_9 is the area ratio A_r/A_a . Equation (A13) is substituted in (A15) to obtain

$$V_a = \frac{K_8 K_9 T}{K_7} \frac{V_r}{T_1} \quad (A16)$$

Substituting equations (A13), (A14), and (A16) in equation (A10),

$$\ln \frac{1 - \frac{N_A}{N_B} \eta_b}{1 - \eta_b} + K_5 = K_3 \frac{(\sigma_A + \sigma_B)^2 (N_B - N_A) e^{-E/RT} LK_7^2 \frac{P_1 T_1}{K_8 K_9 V_r}}{R^{1/2} T^{3/2}} \quad (A17)$$

On the right side of equation (A17) the terms are grouped into: (1) those dependent on fuel type and fuel-air ratio, (2) those dependent on combustor design, and (3) those dependent only on the operating conditions. Substituting (A13), (A14), and (A16) in (A12),

$$\frac{\eta_b}{1 - \eta_b} + K_6 = K_3 \frac{(\sigma_A + \sigma_B)^2 N_B e^{-E/RT} LK_7^2 \frac{P_1 T_1}{K_8 K_9 V_r}}{R^{1/2} T^{3/2}} \quad (A18)$$

Equation (A17) is the general solution, and equation (A18) applies only if the reaction $A+B \rightarrow C+D$ occurs in a zone where $N_A = N_B$. For a given combustor operating with a given fuel at a fixed fuel-air ratio, equation (A17) becomes

$$\ln \frac{1 - \frac{N_A}{N_B} \eta_b}{1 - \eta_b} + K_5 = K_{10} \frac{P_1 T_1}{V_r} \quad (1)$$

For these same conditions, equation (A18) becomes

$$\frac{\eta_b}{1 - \eta_b} + K_6 = K_{11} \frac{P_1 T_1}{V_r} \quad (2)$$

which is applicable only if the bimolecular reaction happens to occur in a zone where $N_A = N_B$. Either equation can be expressed as follows

$$\eta_b = f \frac{P_1 T_1}{V_r} \quad (3)$$

REFERENCES

1. Childs, J. Howard, McCafferty, Richard J., and Surine, Oakley W.: Effect of Combustor-Inlet Conditions on Performance of an Annular Turbojet Combustor. NACA Rep. 881, 1947. (Formerly NACA TN 1357).
2. McCafferty, Richard J.: Effect of Fuels and Fuel-Nozzle Characteristics on Performance of an Annular Combustor at Simulated Altitude Conditions. NACA RM E8C02a, 1948.
3. Getman, Frederick H., and Daniels, Farrington: Outlines of Theoretical Chemistry. John Wiley & Sons, Inc. (New York), 1937.
4. Kassel, Louis S.: The Kinetics of Homogeneous Gas Reactions. Chem. Catalog Co. (New York), 1932.

~~CONFIDENTIAL~~

1353

TABLE I - COMBUSTOR RATING SCALE

Combustor	Critical $P_1 T_1 / \sqrt{r}$ ($\eta_b = 0.85$)
G	5.9×10^3
H	6.0
L	10.7
K	11.3
A	11.9
D	11.9
J	13.8
C	14.0
F	14.3
B	15.9
N	16.4
M	16.7
I	17.8
E	19.0

NACA

~~CONFIDENTIAL~~

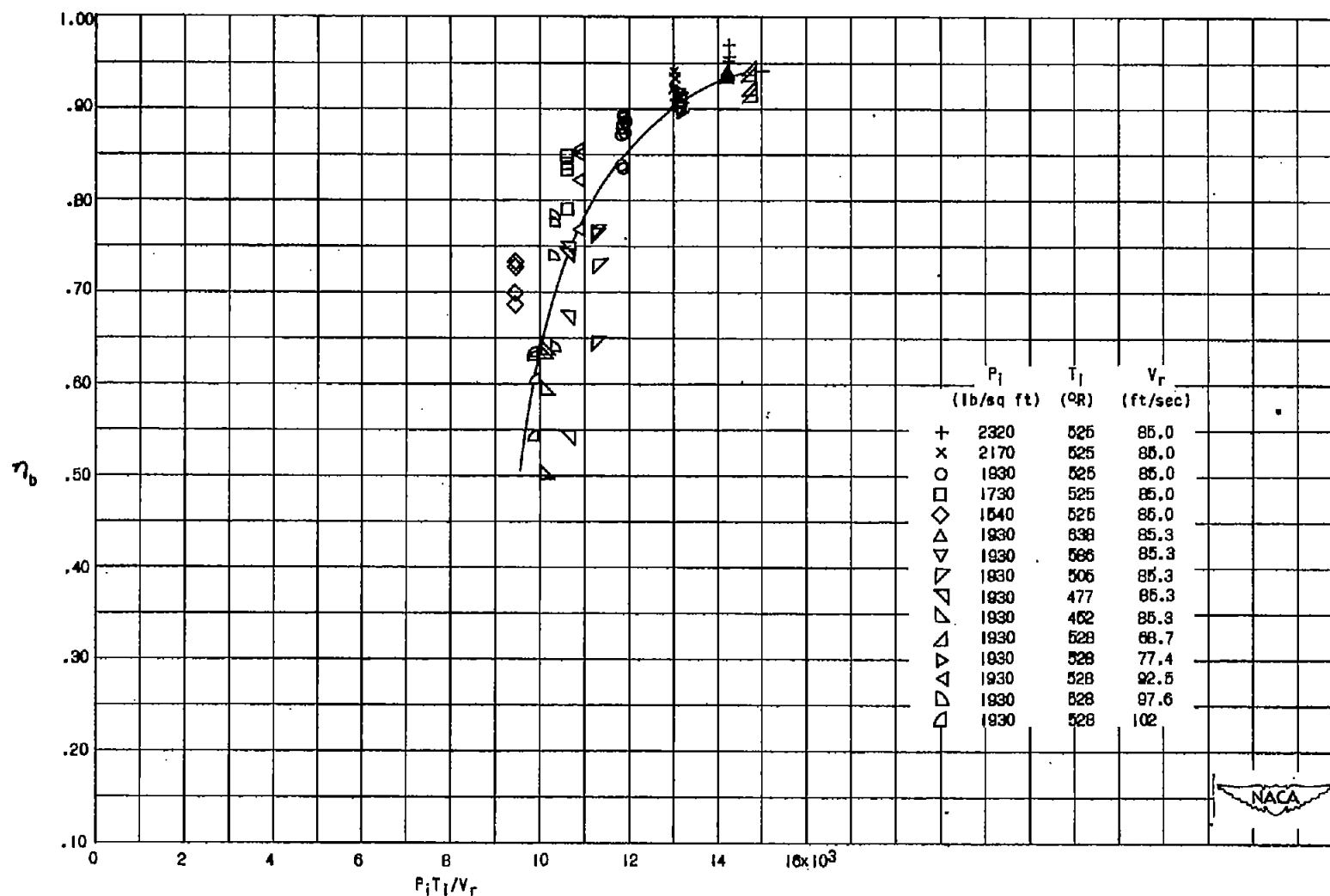


Figure 1. - Experimental data obtained with combustor A (reference 1).
 Fuel, AN-F-22.

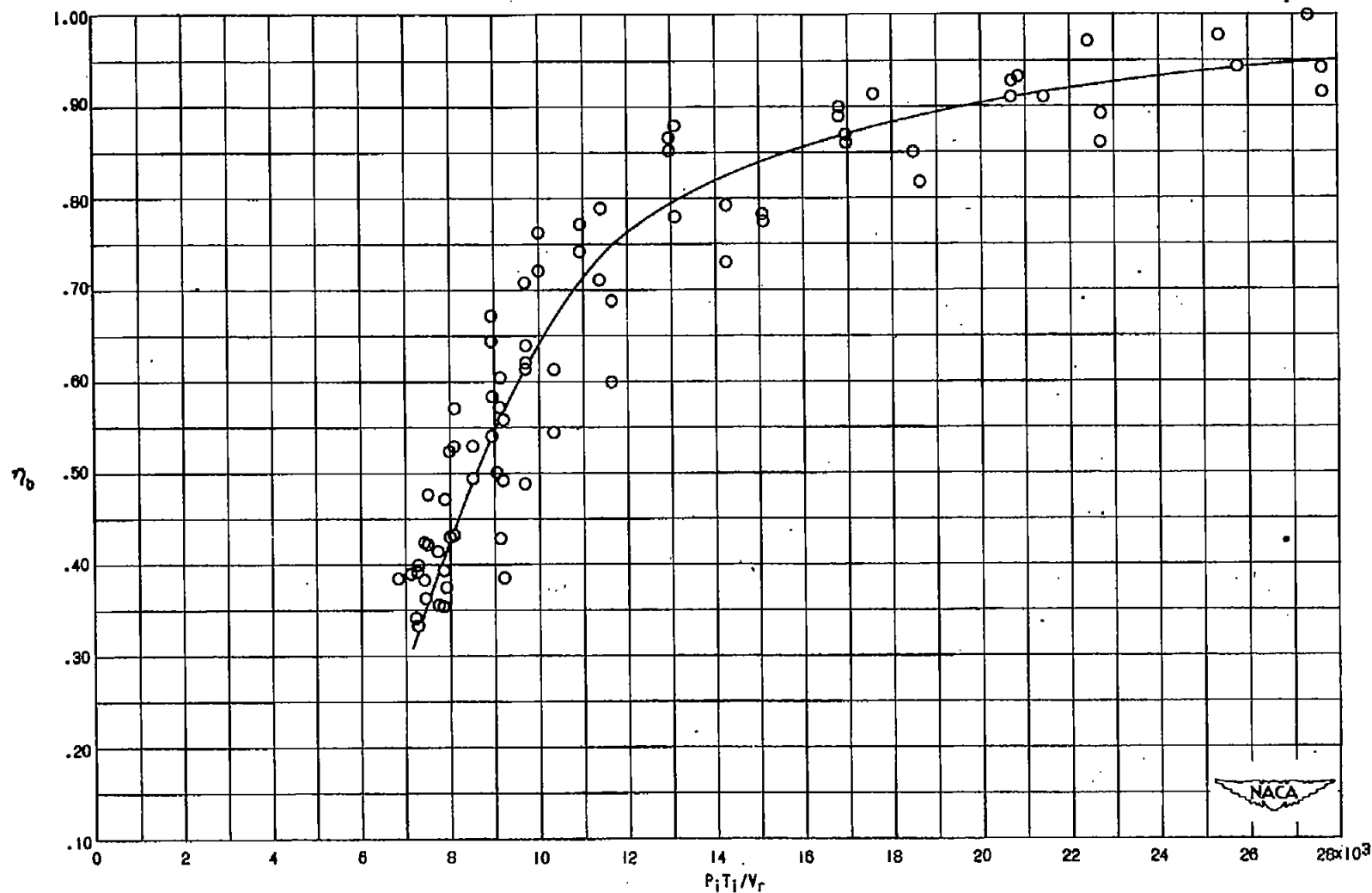
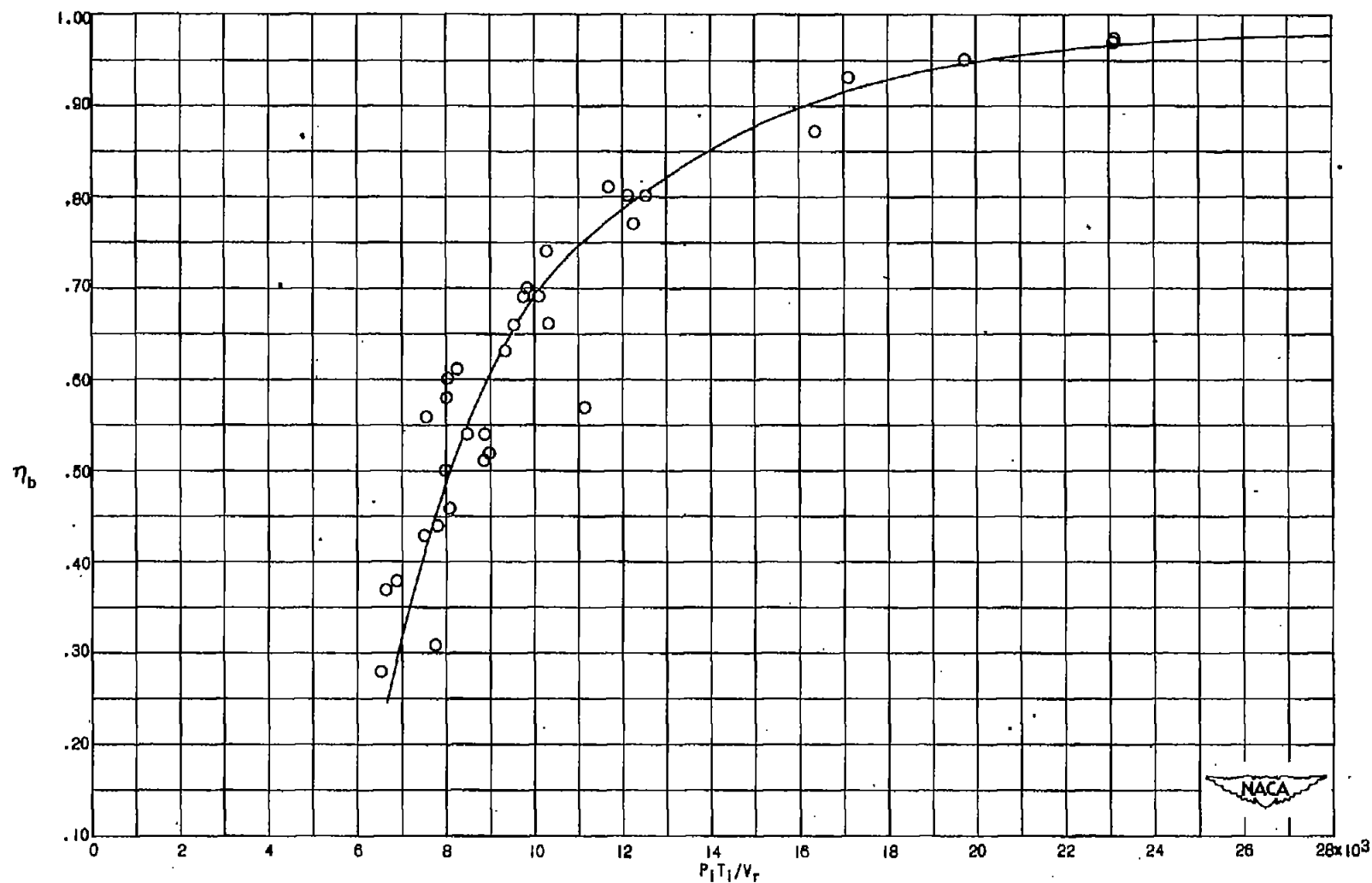
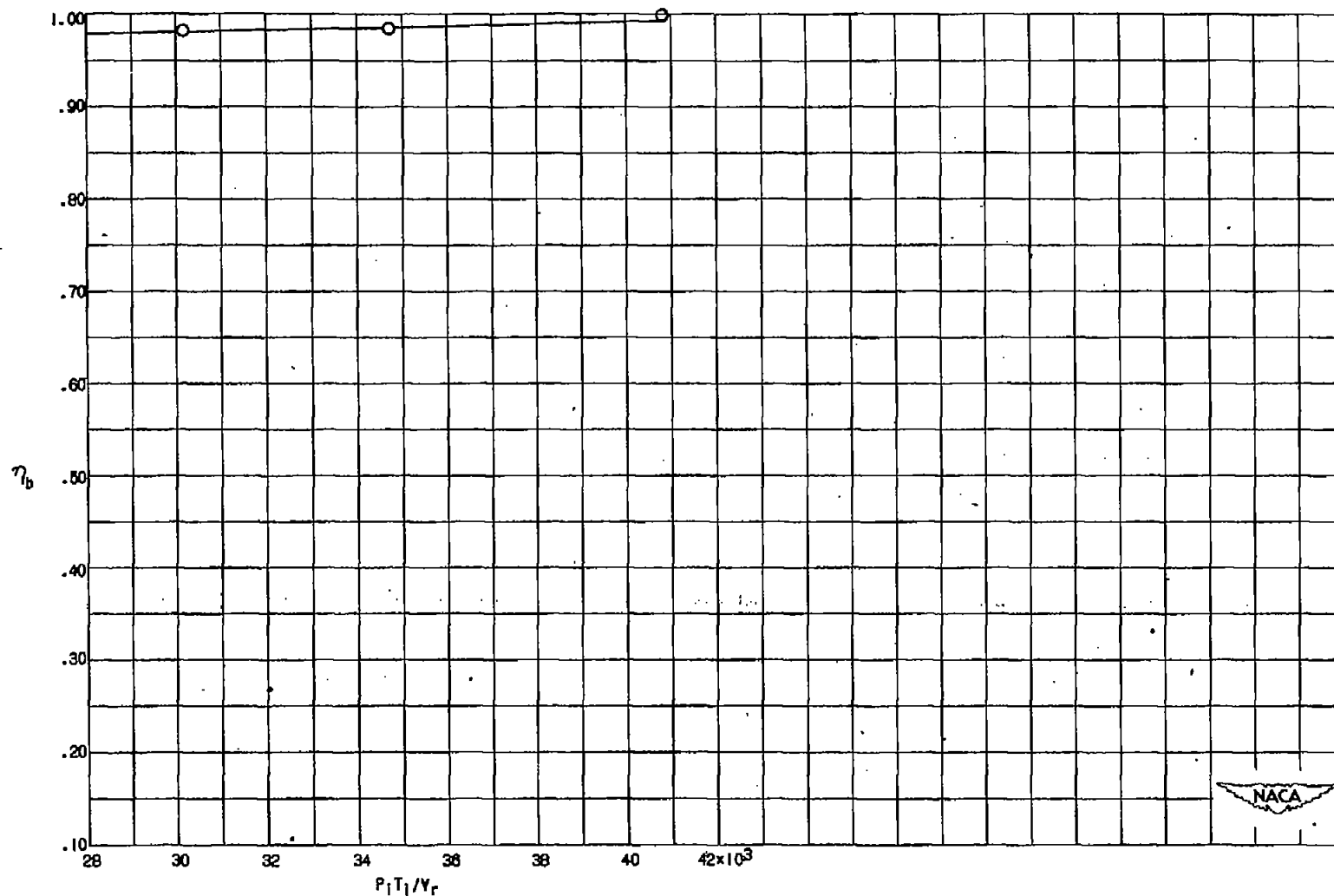


Figure 2. - Experimental data obtained with combustor B. Fuel, AN-F-28.



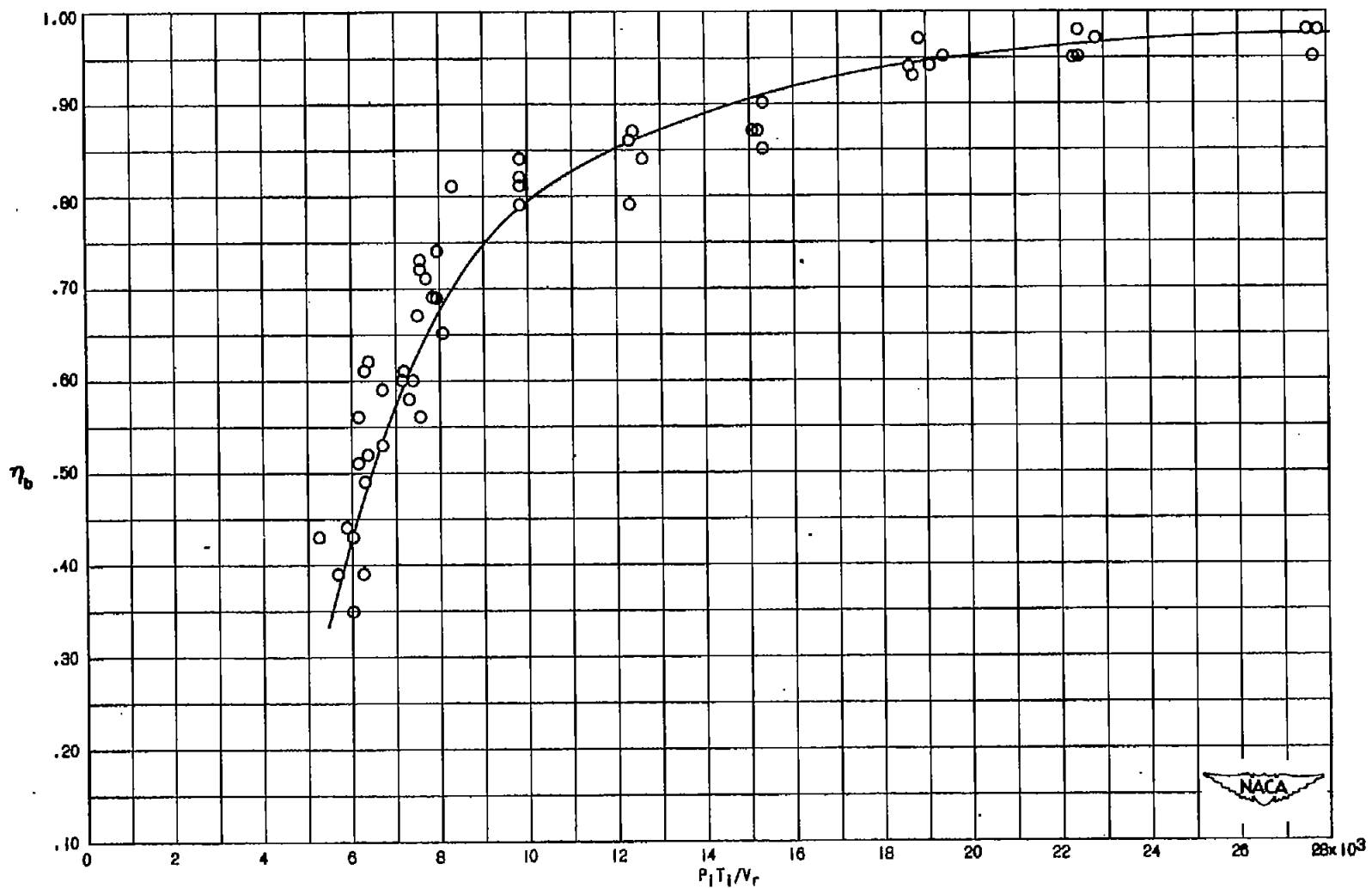
(a) $P_t T_t / V_r < 28 \times 10^3$.

Figure 3. - Experimental data obtained with combustor C. Fuel, AN-F-28.



(b) $P_t T_t / V_r > 28 \times 10^3$.

Figure 3. - Concluded. Experimental data obtained with combustor C.
 Fuel, AN-F-56.

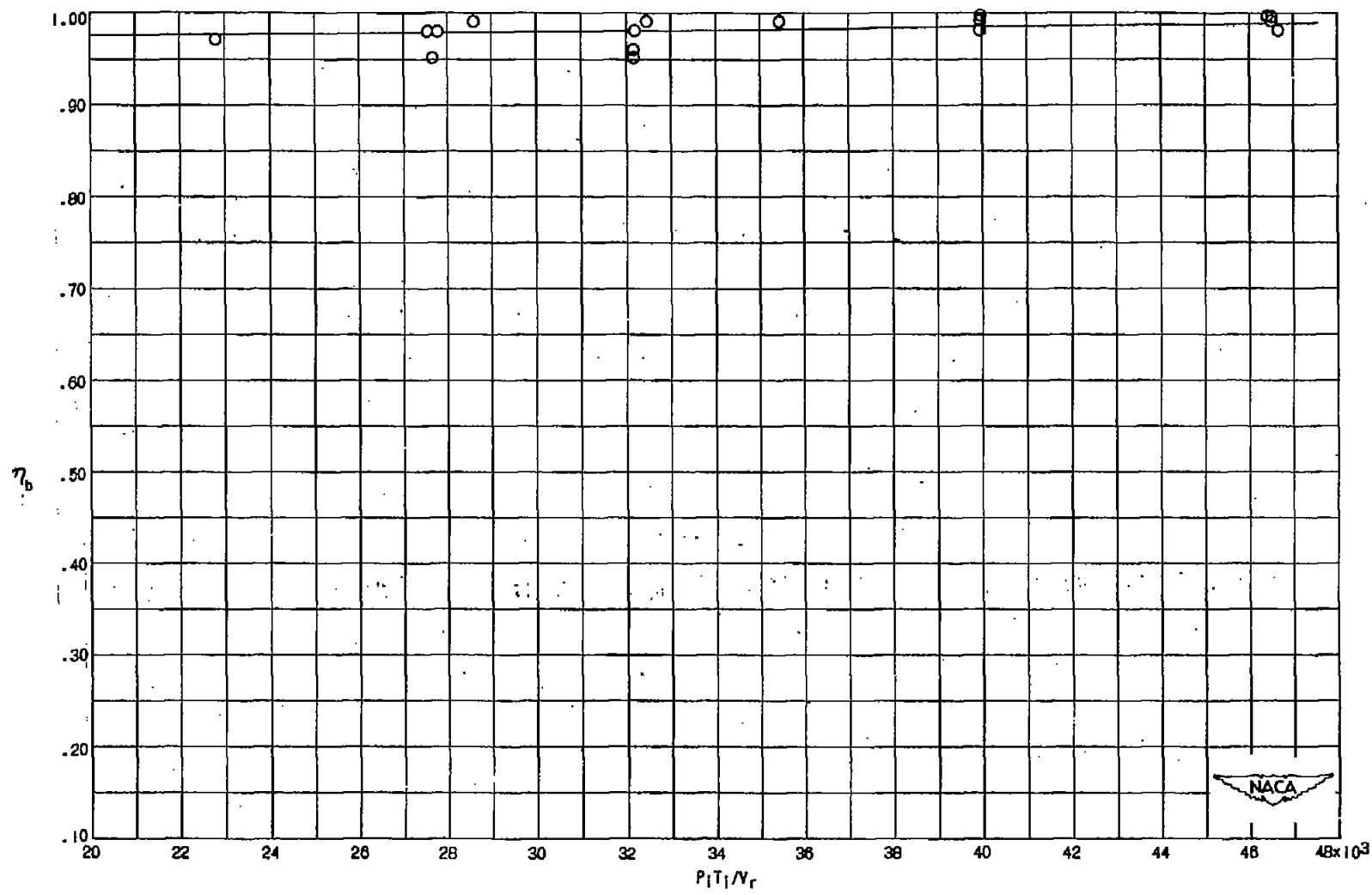


(a) $P_1 T_1 / V_r < 28 \times 10^3$.

Figure 4. - Experimental data obtained with combustor D. Fuel, AN-F-28.

CONFIDENTIAL

CONFIDENTIAL



(b) $P_i T_i / V_r > 20 \times 10^3$.

Figure 4. - Concluded. Experimental data obtained with combustor D. Fuel, AH-F-28.

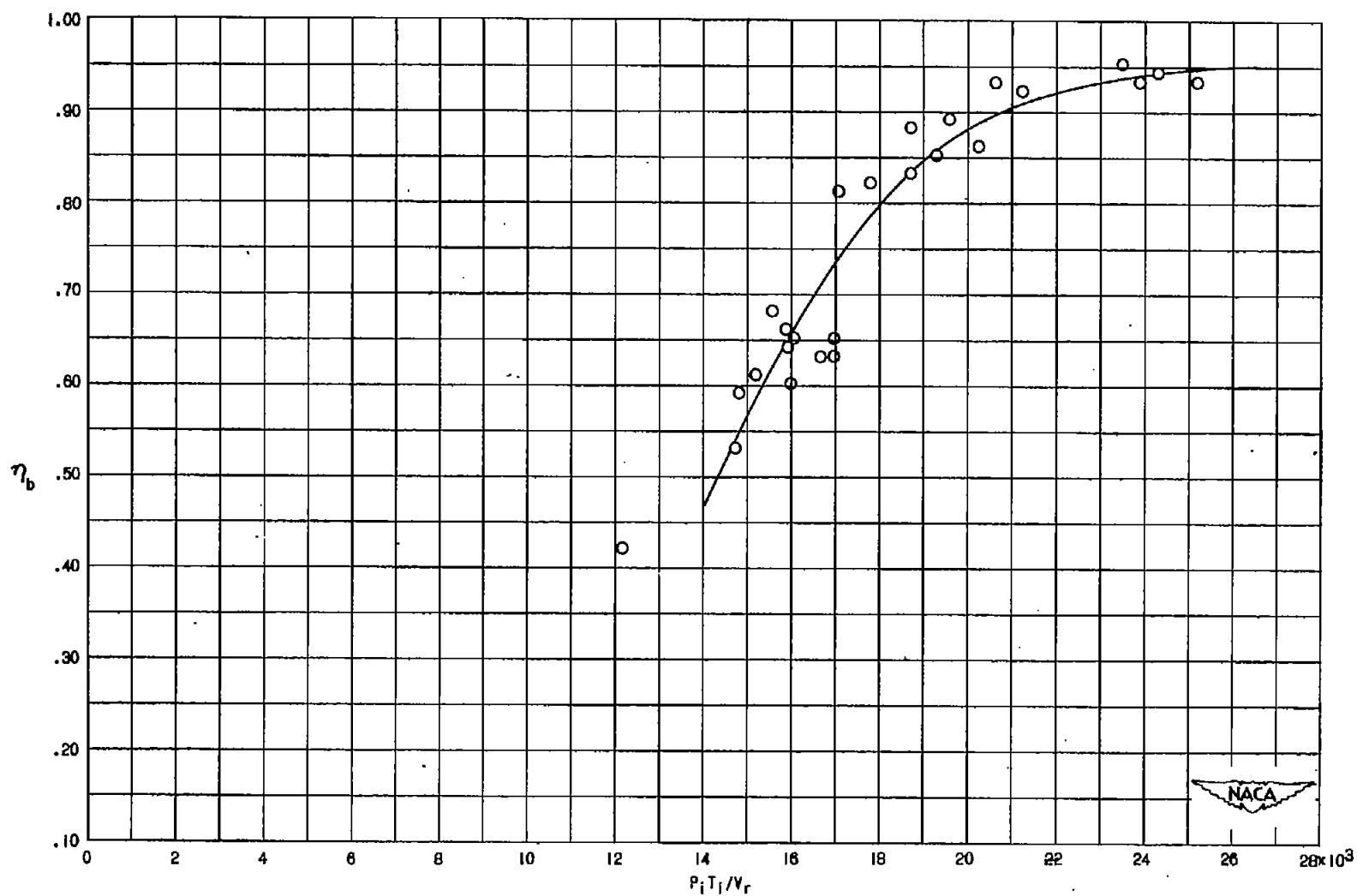


Figure 5. - Experimental data obtained with combustor E. Fuel, AN-F-28.

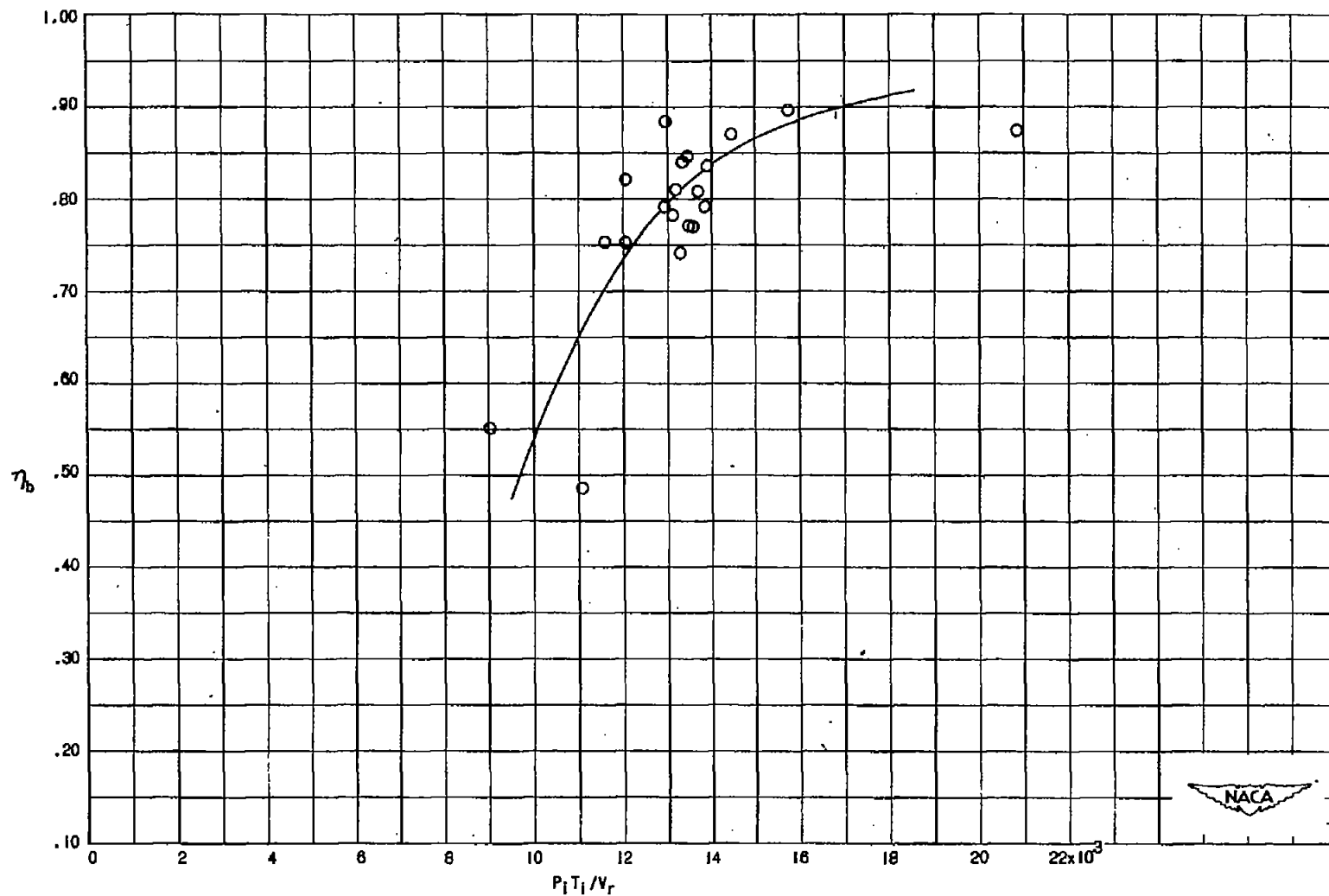


Figure 6. - Experimental data obtained with combustor F. Fuel, AN-F-28.

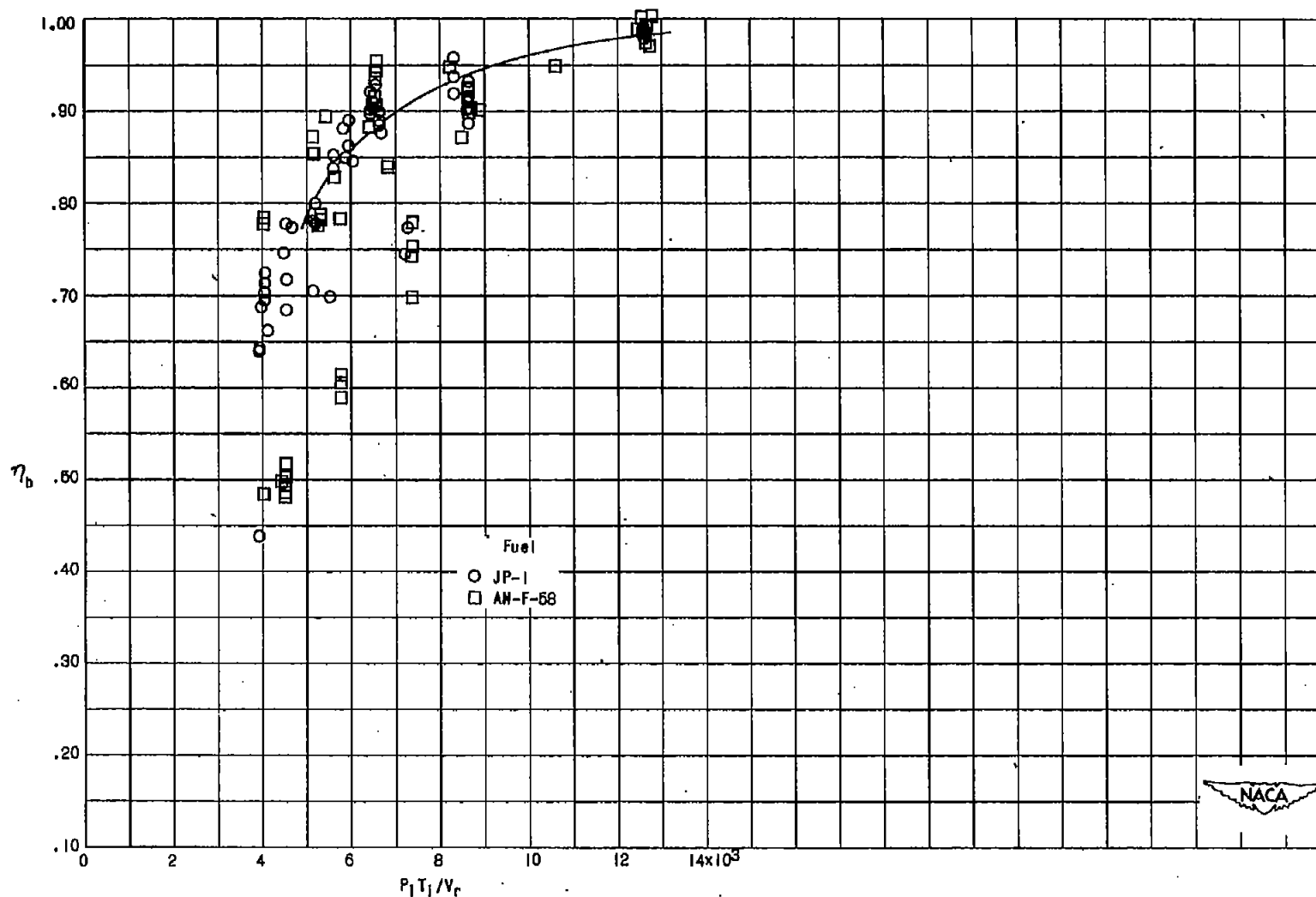


Figure 7. - Experimental data obtained with a single-annulus 25 $\frac{1}{2}$ -inch-diameter combustor of NACA design (combustor G).

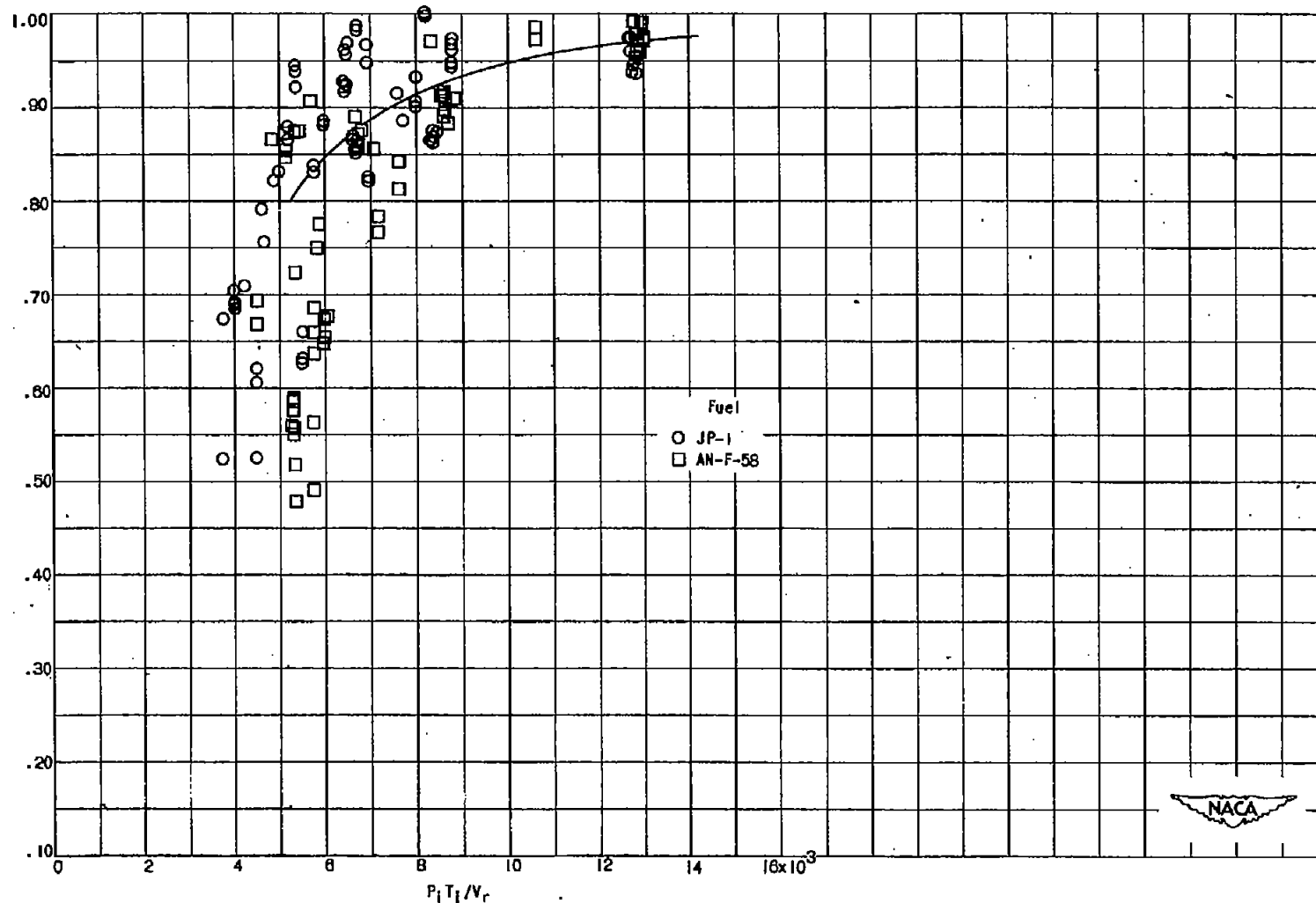
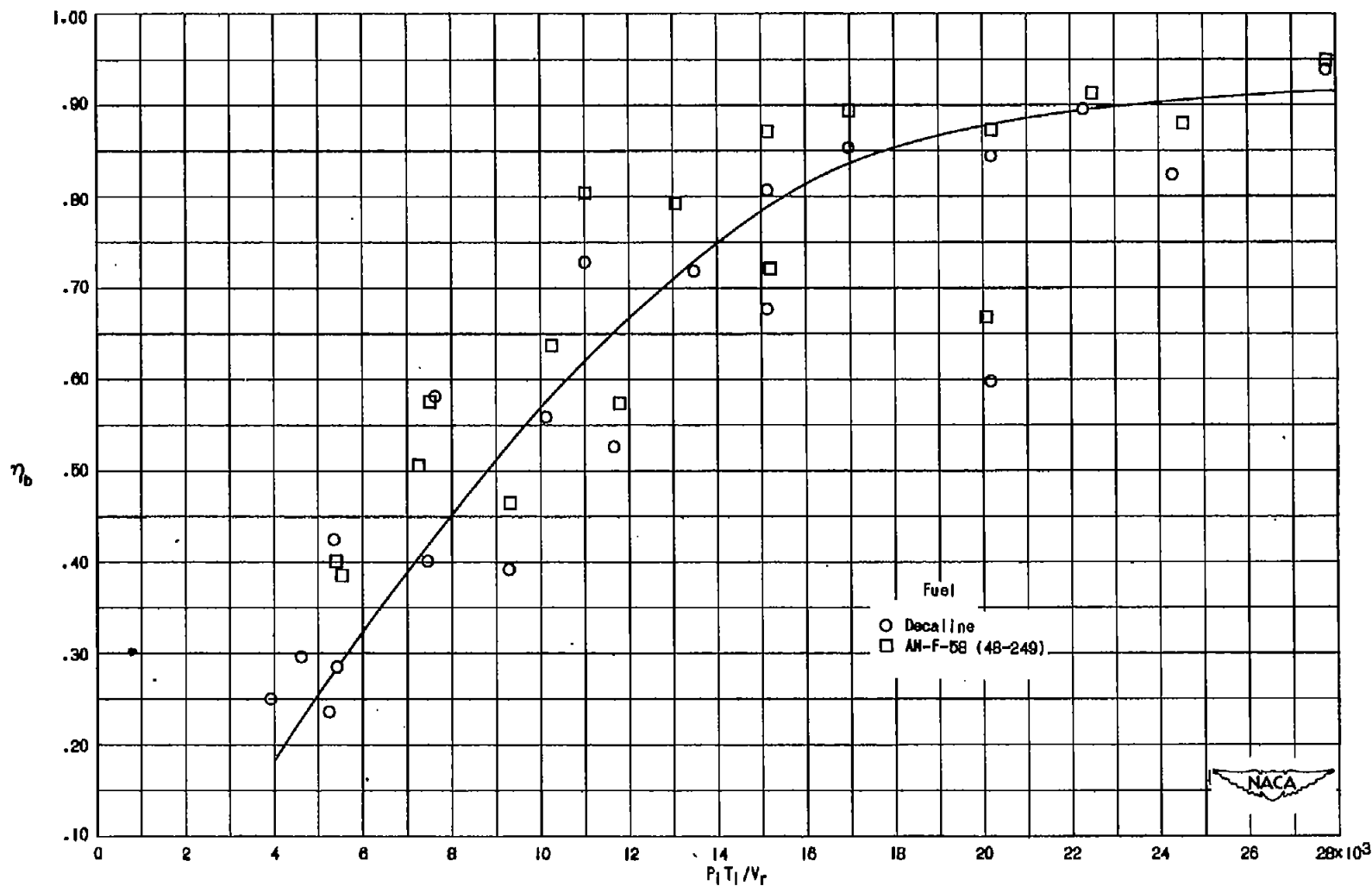
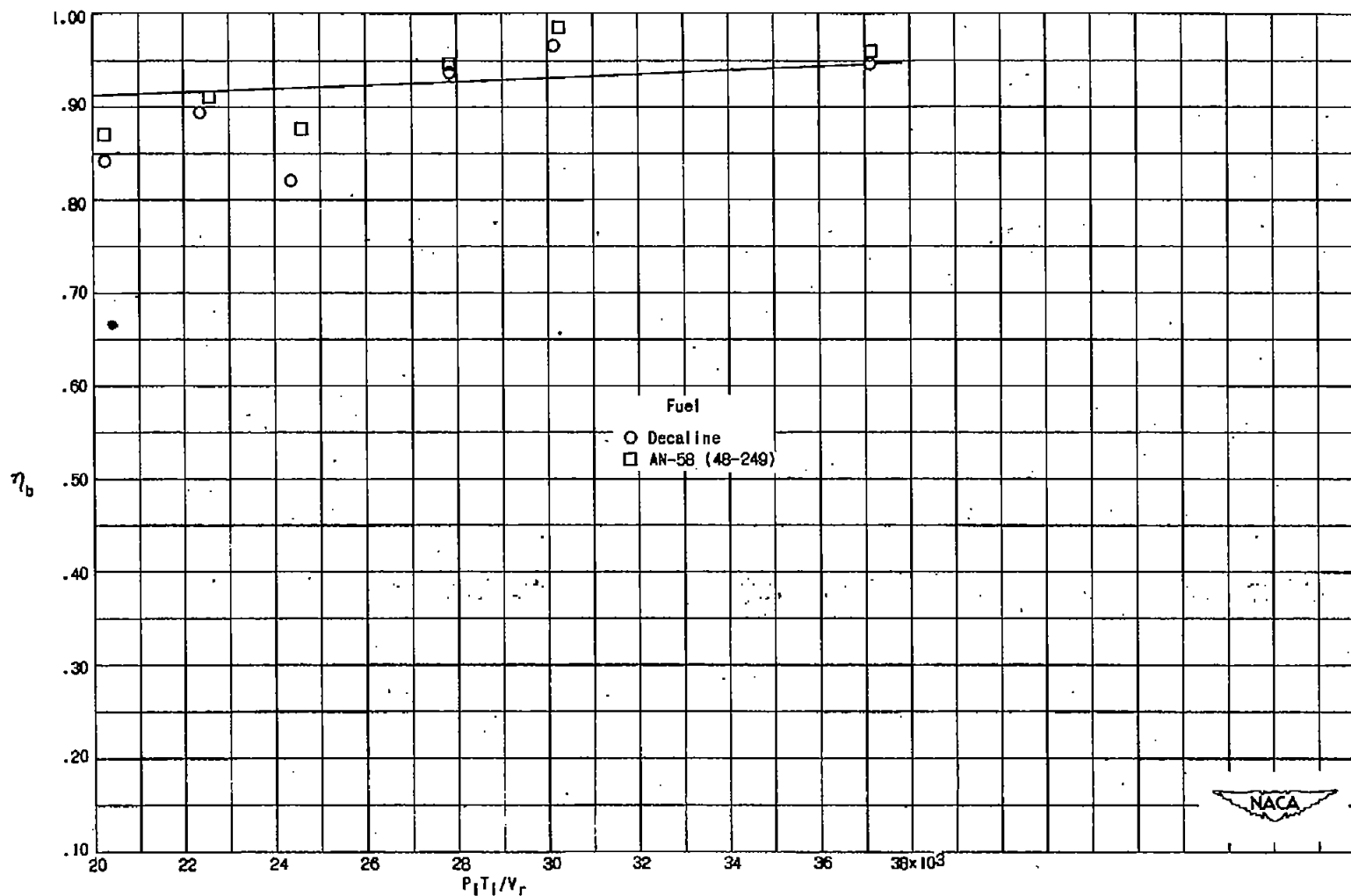


Figure 8. - Experimental data obtained with a single-annulus 25 1/2-inch-diameter combustor of NACA design (combustor H).



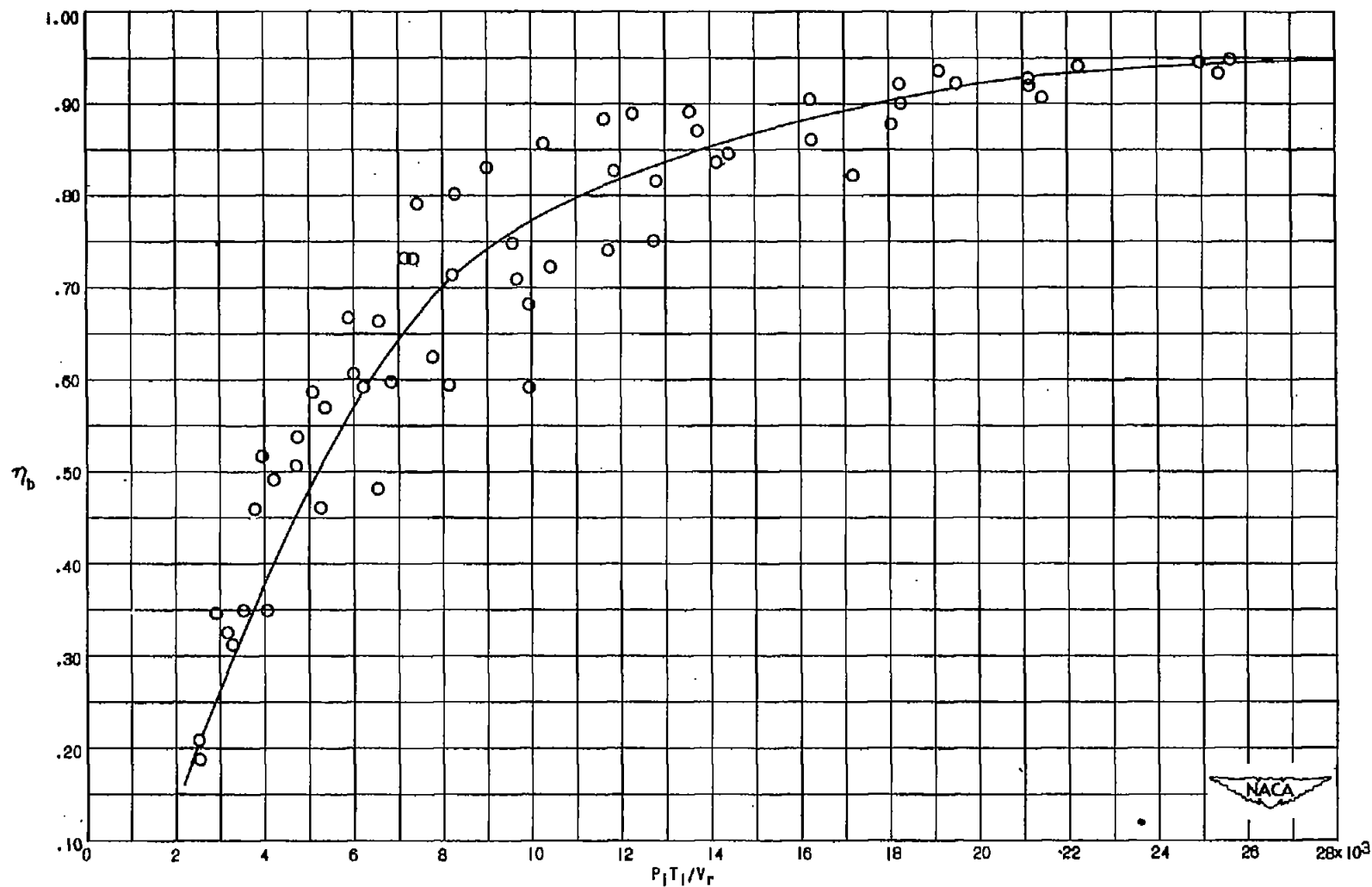
(a) $P_t T_t / V_r < 28 \times 10^3$.

Figure 9. - Experimental data obtained with combustor I.



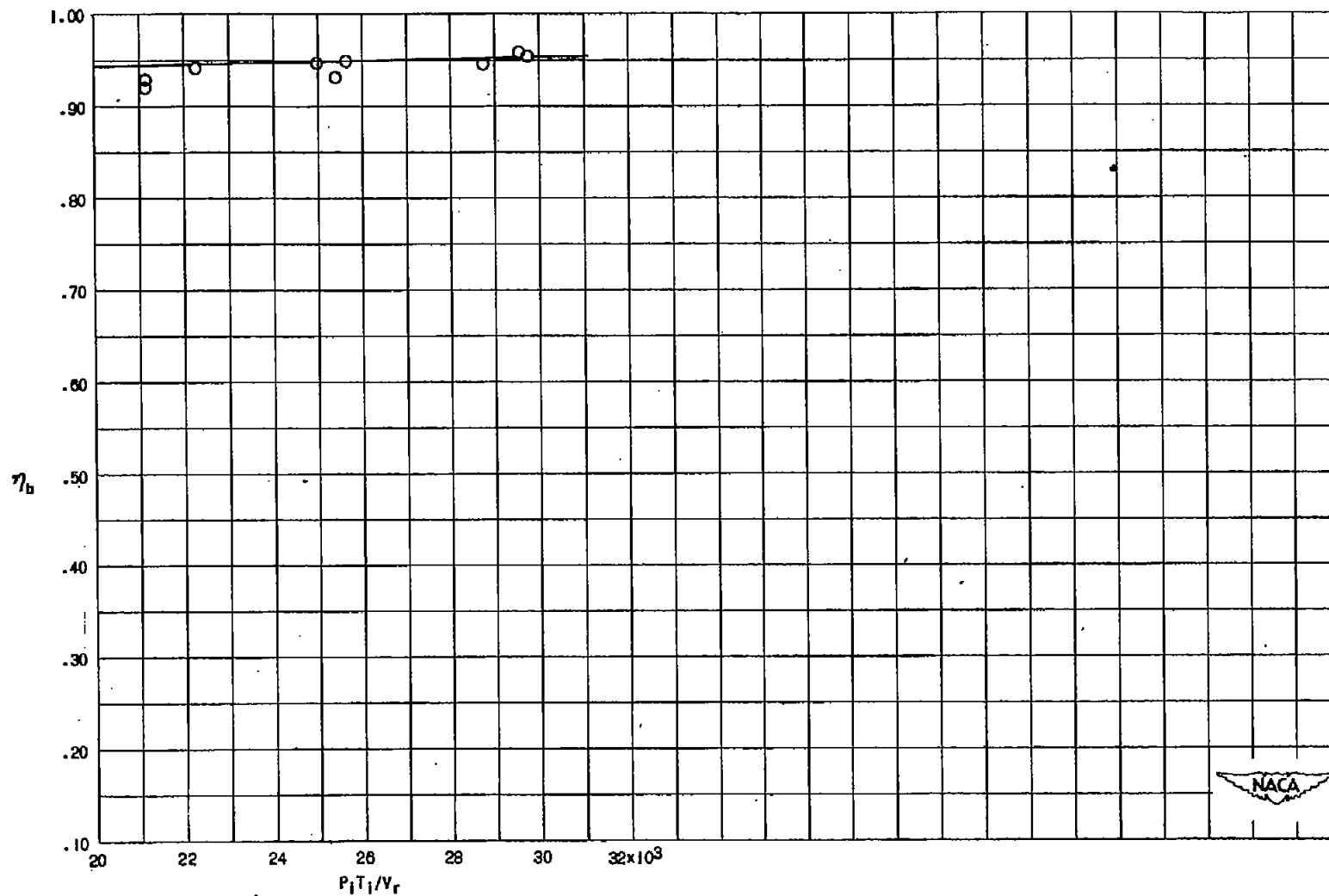
(b) $P_t T_t / V_r > 20 \times 10^3$

Figure 9. - Concluded. Experimental data obtained with combustor I.



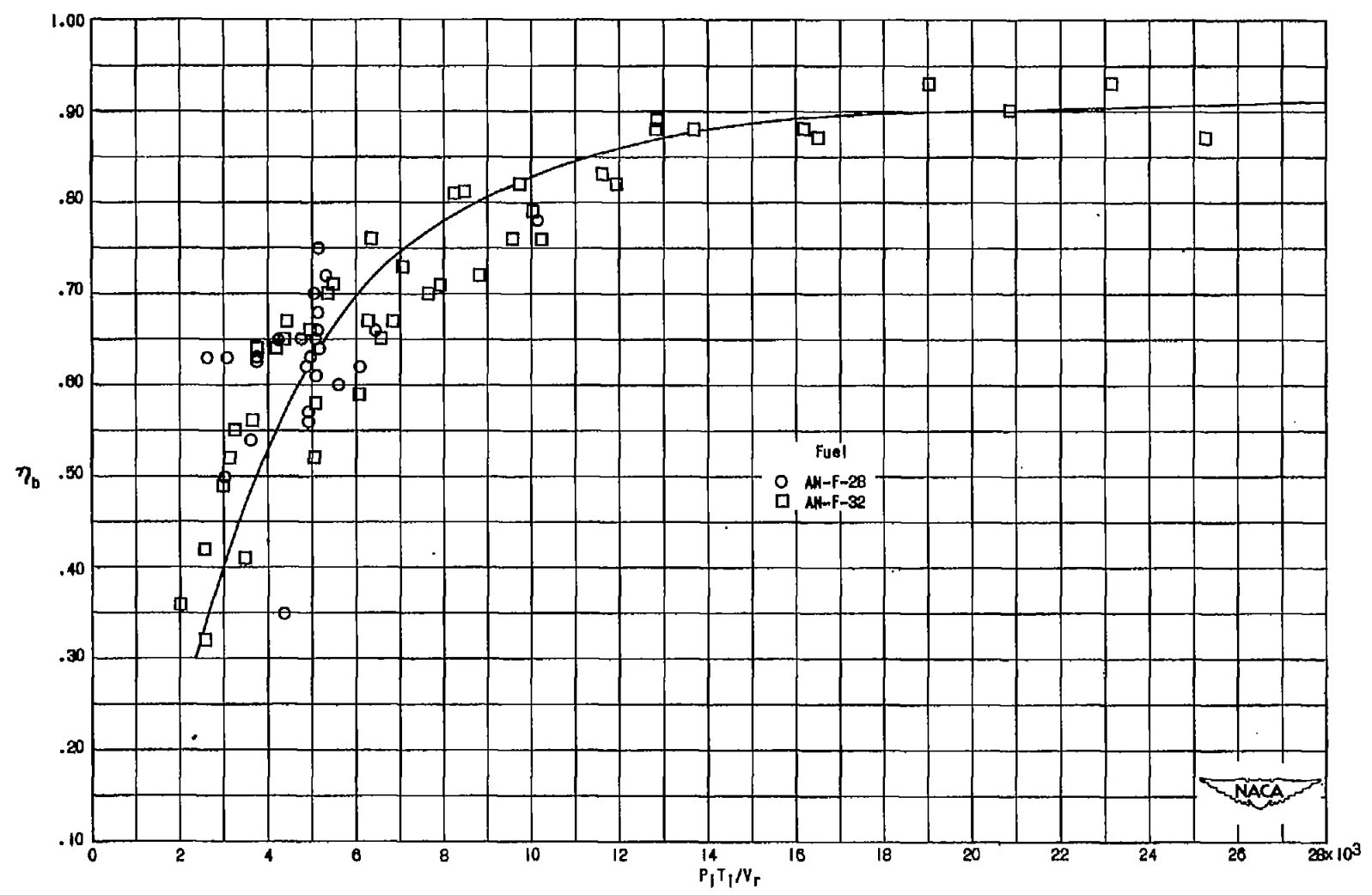
(a) $P_1 T_1 / V_r < 28 \times 10^3$.

Figure 10. - Experimental data obtained with combustor J. Fuel, AN-F-58.



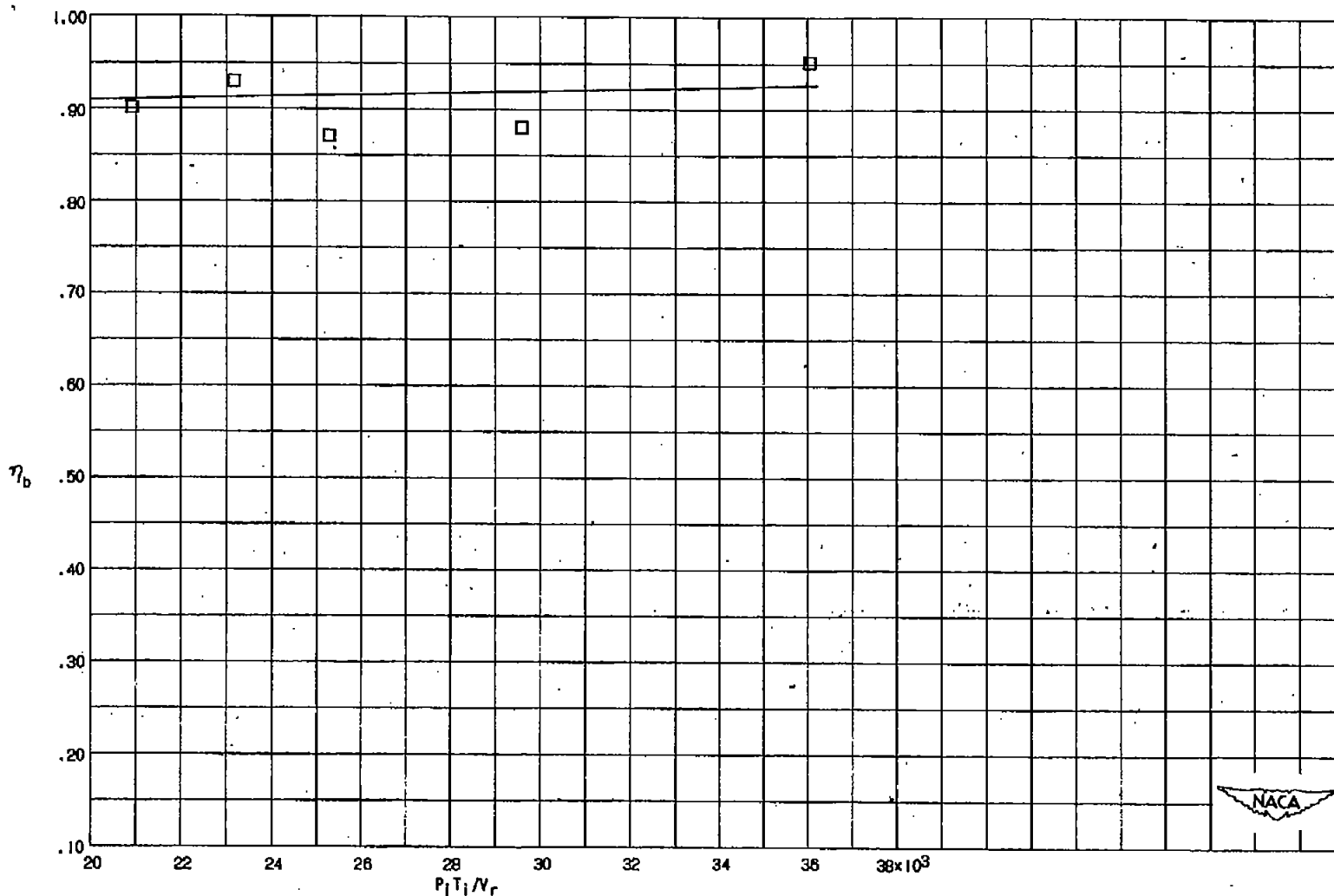
(b) $P_i T_i / V_r > 20 \times 10^3$.

Figure 10. - Concluded. Experimental data obtained with combustor J. Fuel, AN-F-58.



(a) $P_1 T_1 / V_r < 28 \times 10^3$.

Figure 11. - Experimental data obtained with combustor K.



(b) $P_1 T_1 / V_r > 20 \times 10^3$; fuel, AN-F-32.

Figure 11. - Concluded. Experimental data obtained with combustor K.

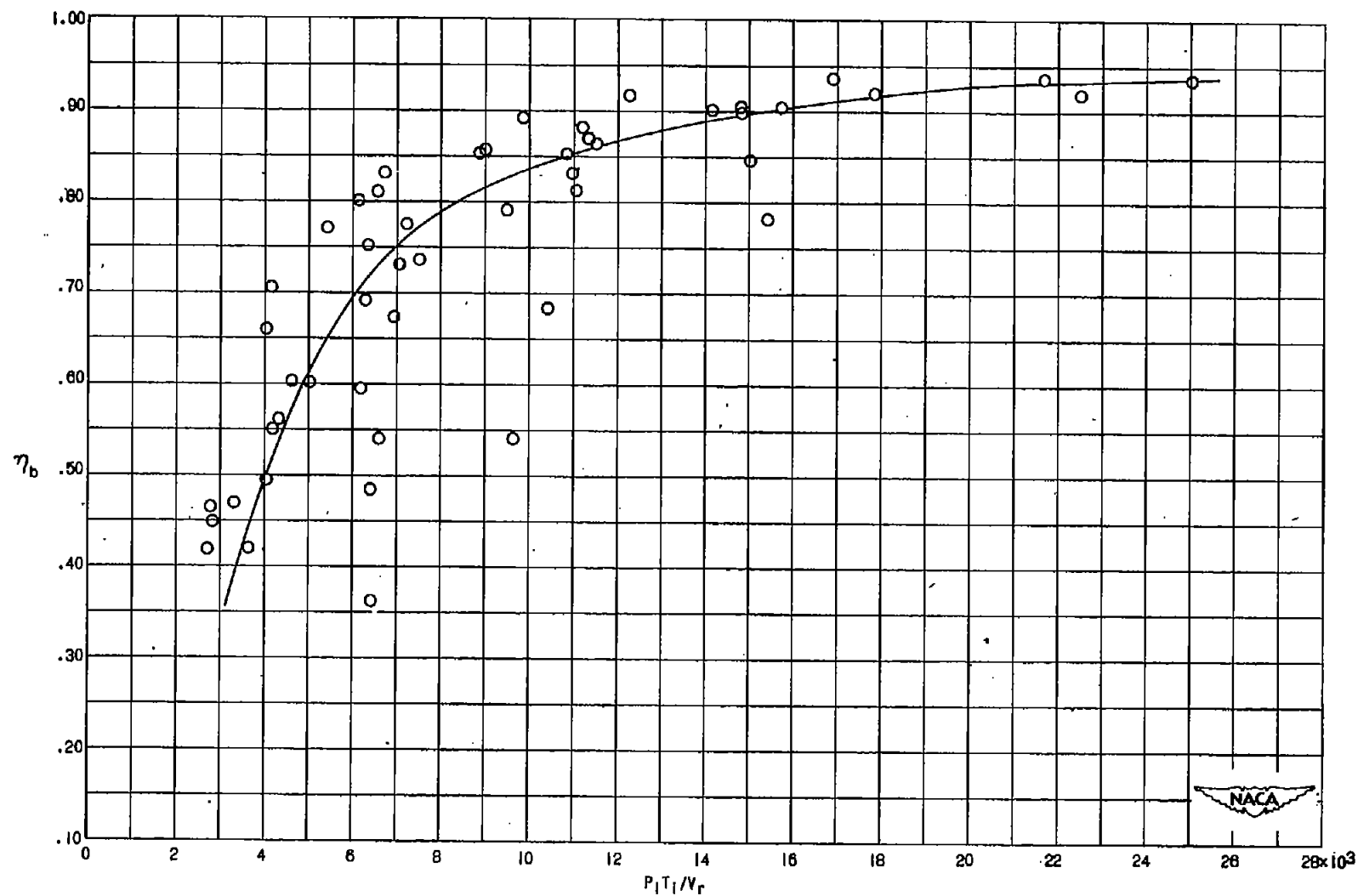


Figure 12. - Experimental data obtained with combustor L. Fuel, AN-F-58.

CONFIDENTIAL

CONFIDENTIAL

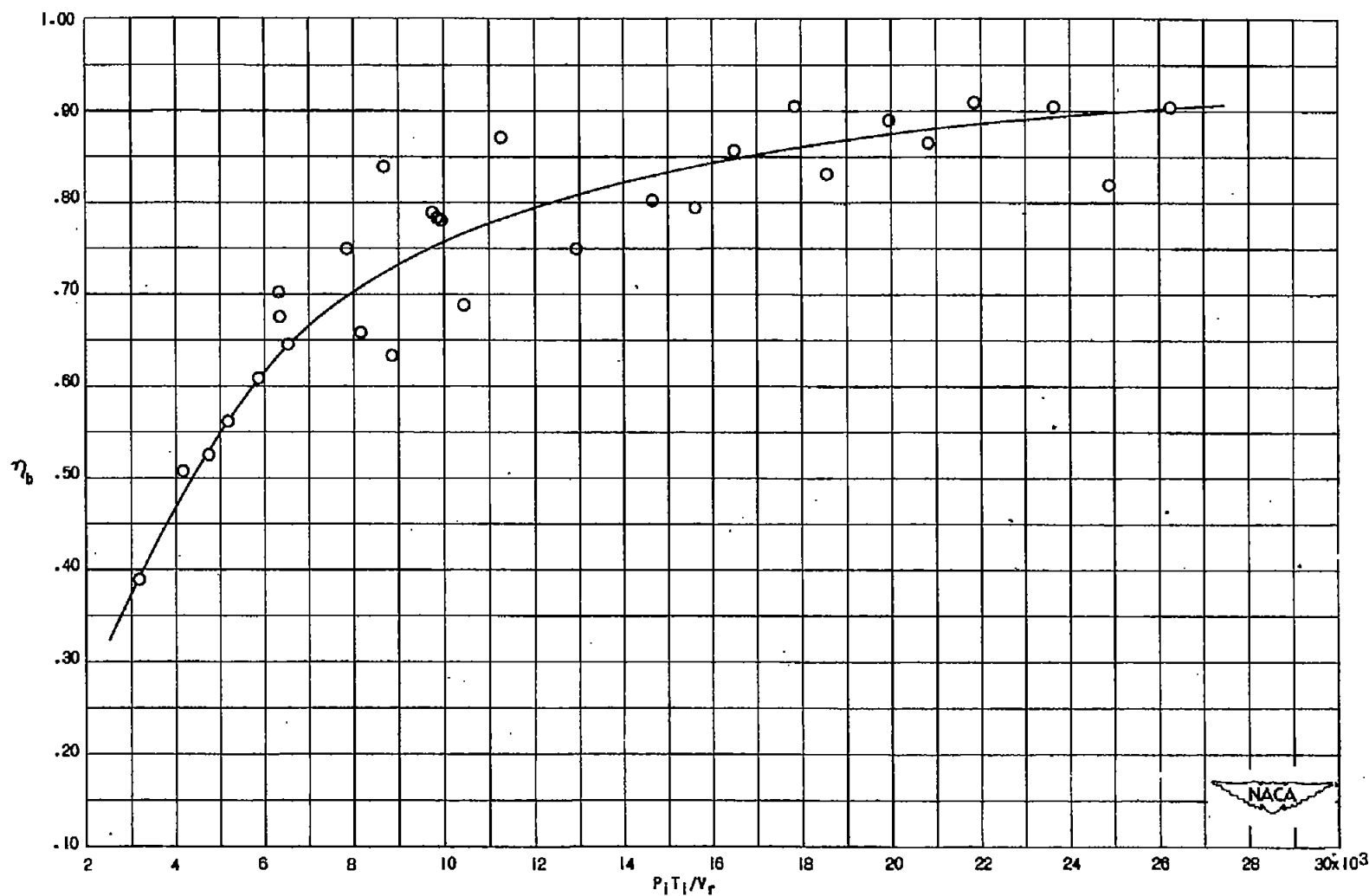
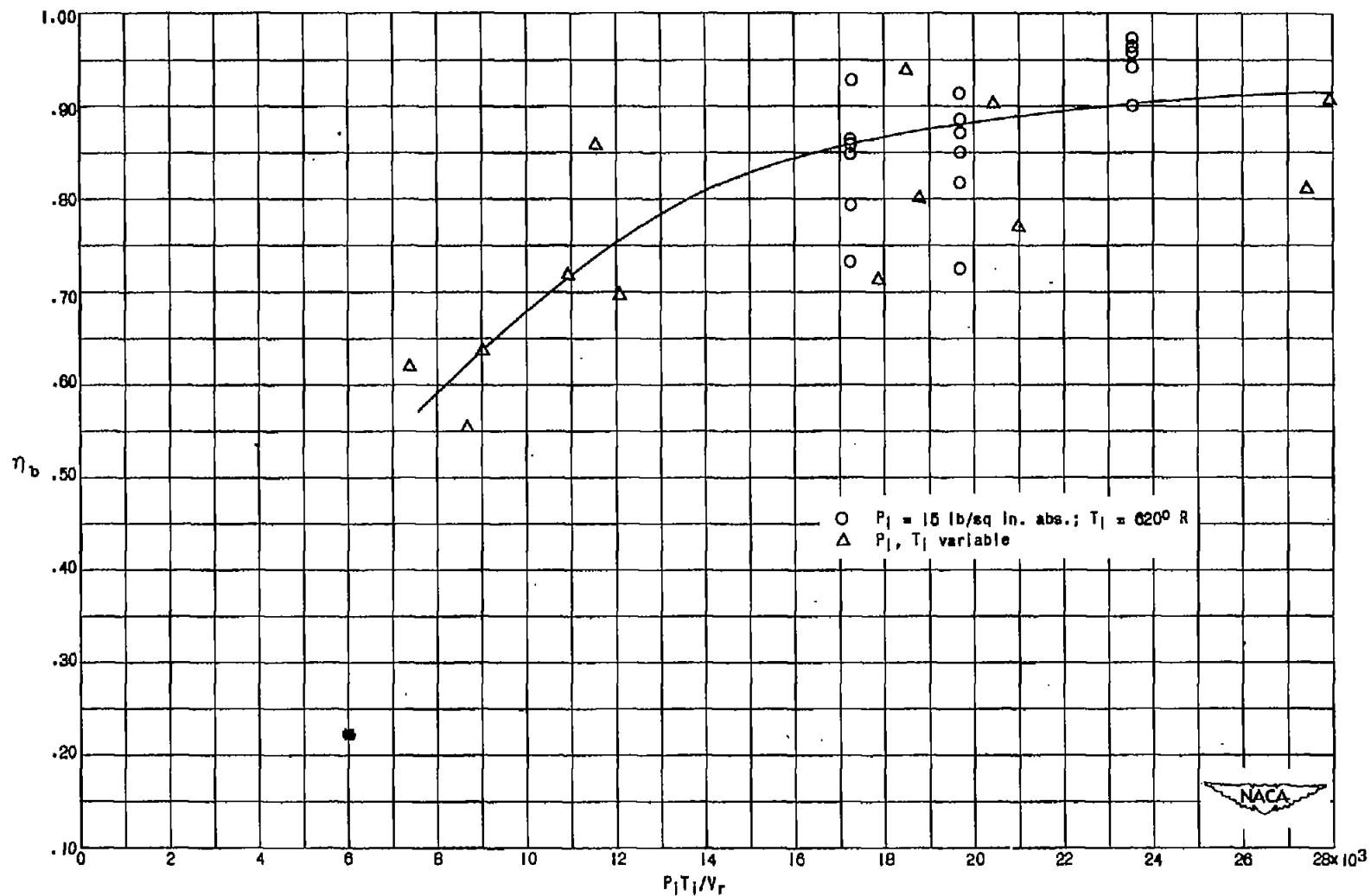
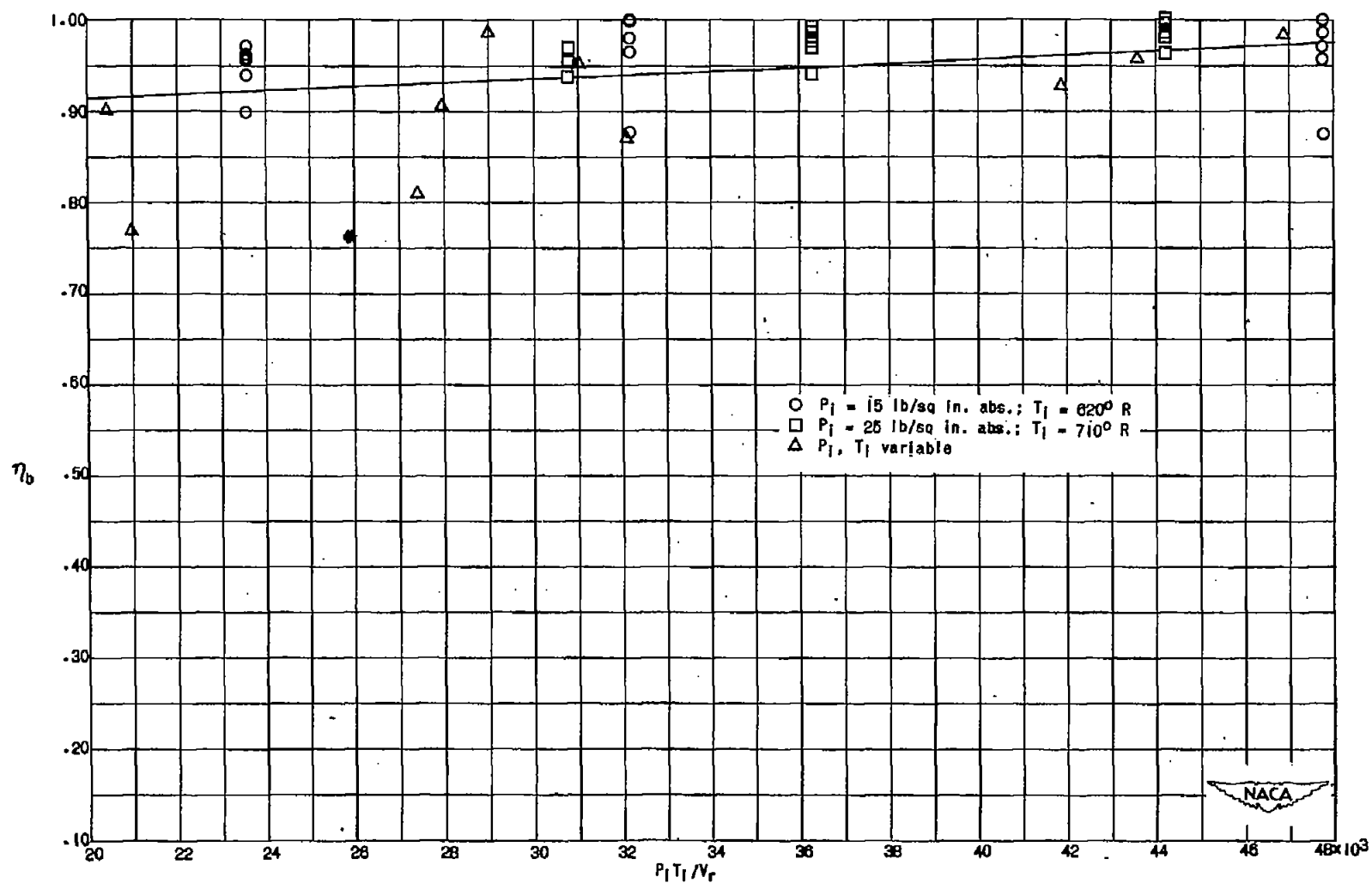


Figure 13. - Experimental data obtained with combustor W.



(a) $P_1 T_1 / V_r < 28 \times 10^3$

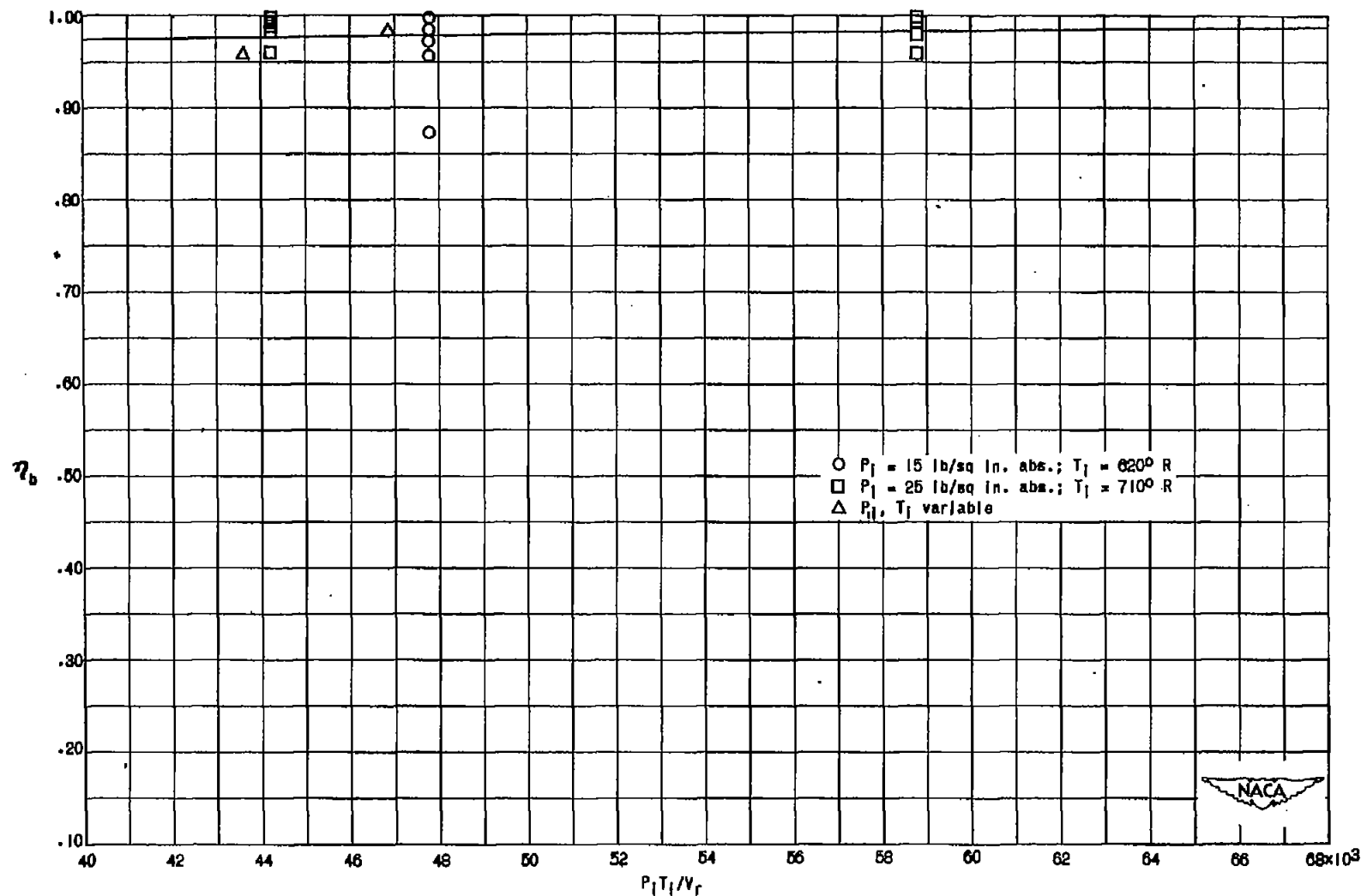
Figure 14. - Experimental data obtained with combustor M. Fuel, AN-F-32.



(D) $20 \times 10^3 < P_1 T_1 / V_r < 48 \times 10^3$.

Figure 14. - Continued. Experimental data obtained with combustor N. Fuel, AN-F-32.

CONFIDENTIAL

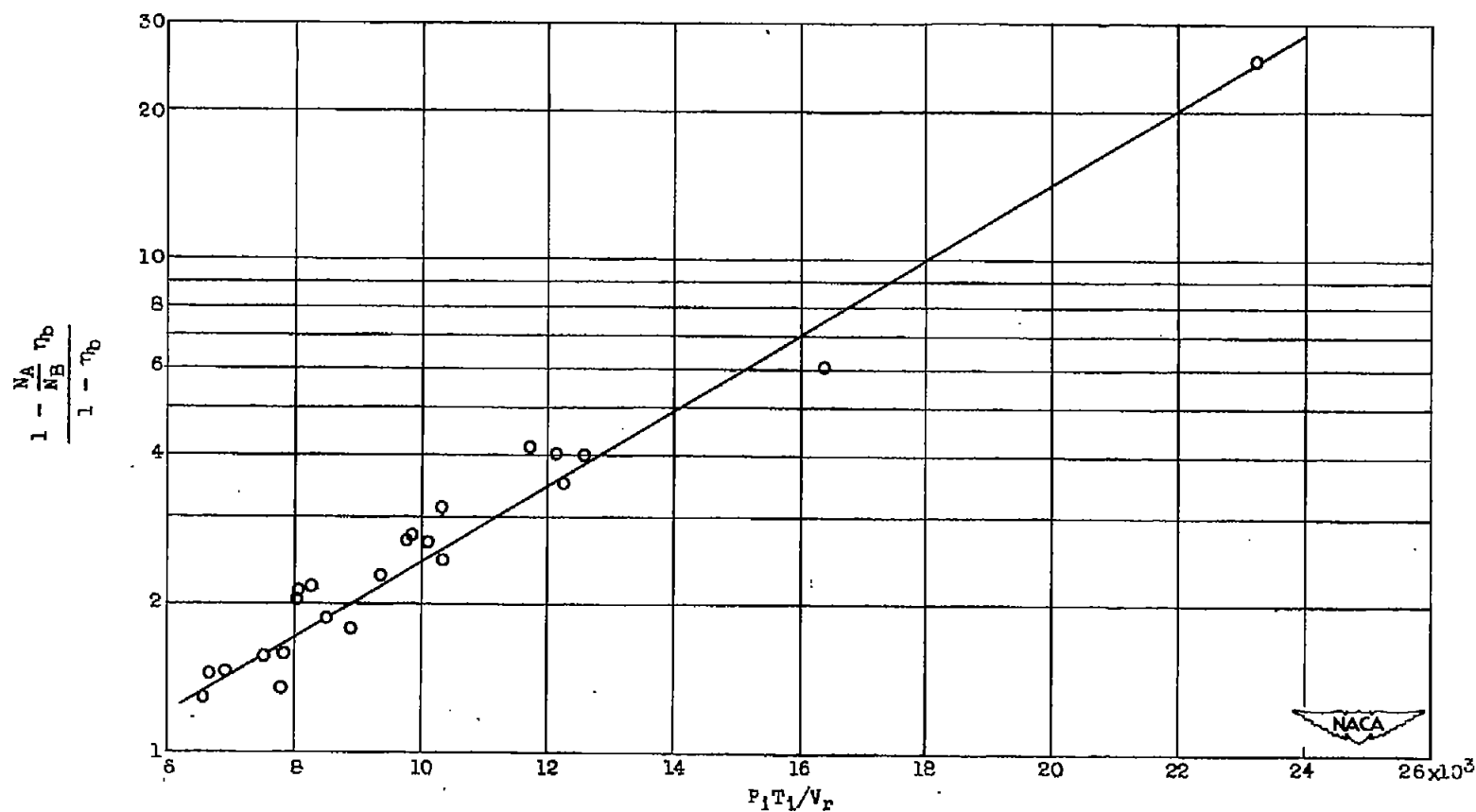


(c) $40 \times 10^3 < P_1 T_1 / V_r < 68 \times 10^3$.

Figure 14. - Concluded. Experimental data obtained with combustor N. Fuel, AN-F-32.

NACA RM E50F15.

CONFIDENTIAL

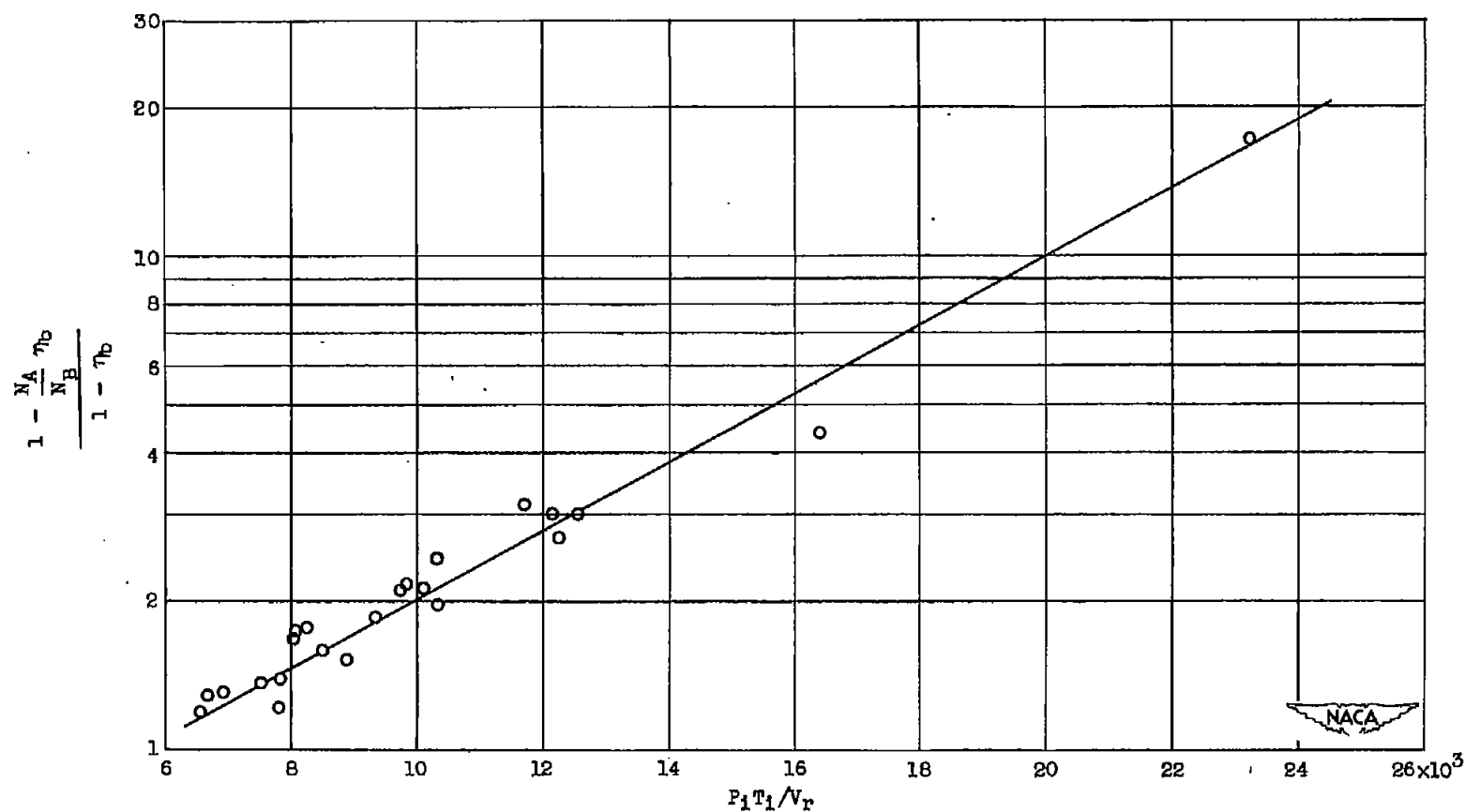


(a) $N_A/N_B = 1/2$.

Figure 15. - Experimental data obtained with combustor C plotted in accordance with equation (1).

1353

NACA RM E50F15.



(b) $N_A/N_B = 1/4$.

Figure 15. - Concluded. Experimental data obtained with combustor C plotted in accordance with equation (1).

~~CONFIDENTIAL~~

NACA RM E50F15.

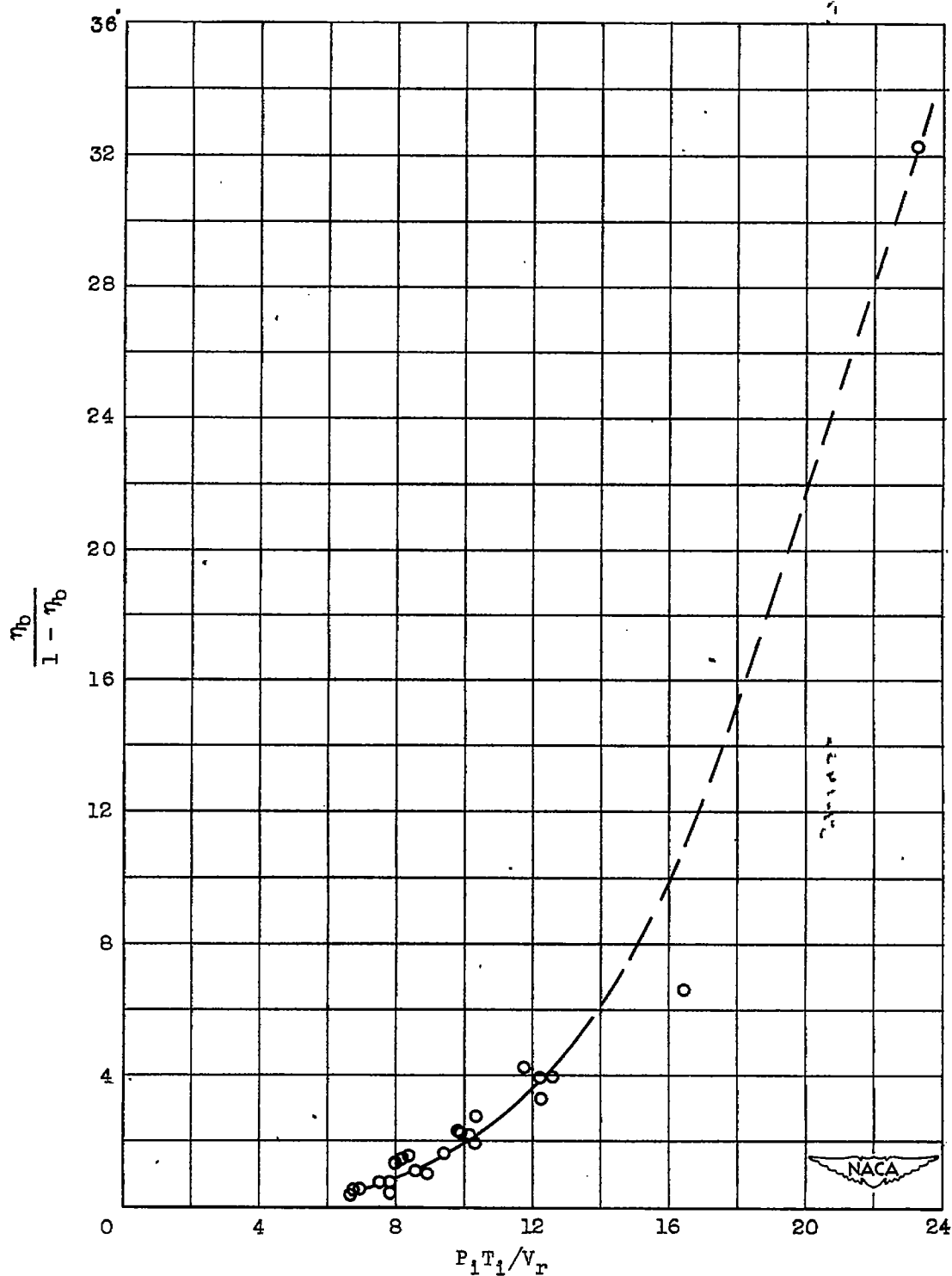


Figure 16. - Experimental data obtained with combustor C plotted in accordance with equation (2).

~~CONFIDENTIAL~~